The Astrophysical Journal, 658:941–959, 2007 April 1


# THE METALLICITY OF GALAXY DISKS: INFALL VERSUS OUTFLOW

Julianne J. Dalcanton[1]
Department of Astronomy, University of Washington, Box 351580, Seattle, WA 98195; jd@astro.washington.edu
*Received 2005 August 16; accepted 2006 August 20*

## ABSTRACT

Both gas accretion (infall) and winds (outflow) change a galaxy's metallicity and gas fraction, lowering the effective yield. Low effective yields in galaxies with rotation speeds $<120$ km s$^{-1}$ have been widely interpreted as due to the onset of supernova-driven winds below a characteristic galaxy mass, but gas accretion is also a viable explanation. However, calculations presented here prove that (1) metal-enriched outflows are the only mechanism that can significantly reduce the effective yield, but only for gas-rich systems; (2) it is nearly impossible to reduce the effective yield of a gas-poor system, no matter how much gas is lost or accreted; and (3) any subsequent star formation drives the effective yield back to the closed-box value. Thus, only gas-rich systems with low star formation rates (such as dwarf irregulars) can produce and maintain low effective yields. The drop in effective yield seen in low-mass galaxies is therefore due to these galaxies' gas richnesses and low star formation rates, which result from their surface densities falling entirely below the Kennicutt SF threshold. Additional calculations confirm that the fraction of baryonic mass lost through winds varies only weakly with galaxy mass, shows no sharp upturn at any mass scale, and does not require that $>15\%$ of the baryons have been lost by galaxies of any mass. Supernova feedback is therefore unlikely to be effective for removing large amounts of gas from low-mass disk galaxies. In addition, the dependence between metal loss and galaxy mass is sufficiently weak that massive galaxies dominate metal enrichment of the IGM. The calculations in this paper provide limiting cases for any arbitrary chemical evolution history, as is proven in an Appendix.

*Subject headings:* galaxies: abundances — galaxies: evolution — galaxies: formation — galaxies: ISM — ISM: evolution

*Online material:* color figures

## 1. INTRODUCTION

Since the seminal work of Larson (1974), supernova-driven winds have been a favored mechanism for explaining the properties of low-mass galaxies. Modern theories of galaxy formation frequently invoke gas outflows (or "feedback") to explain the lack of gas in dwarf spheroidal galaxies (e.g., Sandage 1965; Dekel & Silk 1986; Lanfranchi & Matteucci 2004), the paucity of low-mass galaxies compared to CDM simulations (e.g., White & Frenk 1991), the hot gaseous halos around dwarf starbursts (e.g., Marlowe et al. 1995; Martin 1998; Martin et al. 2002; Ott et al. 2005), and the metal enrichment of the intergalactic medium (e.g., Silk et al. 1987; Madau et al. 2001; Mori et al. 2002).

Outflows may also be partially responsible for low metallicities in disk galaxies, particularly in low-mass dwarf irregulars. For many years there has been evidence for a mass-metallicity relationship among galaxies, with low-mass galaxies having systematically lower metallicities (see Fig. 7 of the review by Pagel & Edmunds 1981 for an early plot of this relation[2]). While some of the correlation between mass and metallicity is certainly due to less past enrichment in gas-rich low-mass galaxies, some may also be due to a direct loss of metals through winds.

Recently, after bringing abundance measurements to a common metallicity scale and fiducial radius, Garnett (2002) found a tight relationship between metallicity and galaxy mass. By combining measurements of the metallicity with estimates of the gas richness, he showed that galaxies systematically depart from the closed-box model of chemical evolution below a characteristic mass scale near $V_c \sim 125$ km s$^{-1}$. These results have since been qualitatively confirmed by Pilyugin et al. (2004), using an alternative abundance calibration, and by Tremonti et al. (2004), using a much larger sample of metallicities from the Sloan Digital Sky Survey (SDSS), although with less accurate gas mass fractions. These results have widely been interpreted as evidence for the onset of strong galactic winds at a specific galaxy mass scale, below which gas and metals can easily escape the shallow potential well.

Although most theoretical attention has focused on outflow, infall is an equally appealing mechanism for producing low metallicities. Outflow reduces the metallicity by preferentially driving metals out of a system, while infall reduces the metallicity by diluting a galaxy's interstellar medium (ISM) with fresh, low-metallicity gas. As shown by Köppen & Edmunds (1999), the metallicity drops if the rate of infall is higher than the rate of star formation, thus allowing the accreted metal-poor gas to dilute the ISM faster than it can be enriched by evolving stars. Given the very low star formation rates and star formation efficiencies seen in the majority of low-mass disk galaxies (e.g., Hunter & Elmegreen 2004), infall is therefore a viable mechanism for producing low metallicities in low-mass galaxies.

The conclusion that low-mass galaxies have not evolved as "closed boxes" is based on measurements of their effective yields. The effective yield measures how a galaxy's metallicity deviates from what would be expected for a galaxy that had the same gas mass fraction, but that had been evolving as a closed box; that is, with no inflow or outflow of gas. A system that evolves as a closed box obeys a simple analytic relationship between the metallicity of the gas and the gas mass fraction (see reviews by Pagel 1997 and Tinsley 1980). As gas is converted into stars, the gas mass

[1] Alfred P. Sloan Foundation Fellow.

[2] While outflow was initially considered as a possible explanation for the mass-metallicity relationship in disks, most initial theoretical work on outflows focused primarily on elliptical systems (e.g., Hartwick 1980).

fraction $f_{\rm gas}$ [$\equiv M_{\rm gas}/(M_{\rm gas}+M_{\rm stars})$] decreases and the metallicity $Z_{\rm gas}$ of the gas increases according to (Searle & Sargent 1972)

$$Z_{\rm gas} = y_{\rm true} \ln (1/f_{\rm gas}), \quad (1)$$

where $y_{\rm true}$ is the true nucleosynthetic yield, defined as the mass in primary elements freshly produced by massive stars, in units of the stellar mass that is locked up in long-lived stars and stellar remnants. For closed-box evolution, the metallicity increases without limit and equals the nucleosynthetic yield when $f_{\rm gas} = \exp(-1)$. Equation (1) assumes that the metals produced by a generation of stars are instantly returned to the ISM and are well mixed with existing gas. This "instantaneous recycling" approximation is likely to be valid for measurements of galaxies' current gas-phase metallicities, which typically use oxygen abundances measured in H II regions. Since the production of oxygen is dominated by winds and supernovae (SNe) from massive stars (>8 $M_\odot$; see Figs. 5 and 7 from Maeder 1992), prompt return of oxygen to the local ISM is a reasonable assumption.

If a galaxy evolves as a closed box, the ratio of $Z_{\rm gas}/\ln f_{\rm gas}^{-1}$ should be a constant equal to the nucleosynthetic yield. However, this ratio will be lower if metals have been lost from the system through winds, or if the current gas has been diluted with fresh infall of metal-poor gas. One may therefore define the above ratio as the "effective yield,"

$$y_{\rm eff} \equiv \frac{Z_{\rm gas}}{\ln (1/f_{\rm gas})}, \quad (2)$$

which will be constant ($y_{\rm eff} = y_{\rm true}$) for any galaxy that has evolved as a closed box, assuming that the nucleosynthetic yield is invariant. In contrast, if any gas has either entered or left the galaxy, the measured effective yield will drop[3] below the closed-box value of $y_{\rm eff} = y_{\rm true}$, due to changes in the metallicity $Z_{\rm gas}$ and/or the gas mass fraction $f_{\rm gas}$. The effective yield is therefore an observationally determined quantity that can be used to diagnose departures from closed-box evolution.

Unfortunately, low values of $y_{\rm eff}$ alone do not immediately reveal *why* a system has departed from closed-box evolution. Either the addition of metal-poor gas or the removal of metal-rich gas could suppress the measured effective yield. It is therefore premature to assume that supernova-driven outflows alone can explain the low effective yields seen for galaxies with $V_c \lesssim 100$–$120$ km s$^{-1}$.

This paper explores ways to distinguish between infall and outflow using the effective yield and the gas mass fraction. Section 2 summarizes the current observations of effective yields. Calculations in § 3 show how infall (§ 3.1), outflow (§ 3.2), and the subsequent return to closed-box evolution (§ 3.3) change the effective yield and the gas mass fraction. A comparison with observational data in § 4 leaves metal-rich outflows as the only viable mechanism for producing the low effective yields observed in gas-rich galaxies. Section 5 stresses the importance of high gas richness in allowing enriched outflows to suppress the effective yield and suggests that the observed mass-dependent threshold in the effective yield is more closely linked to low star formation efficiencies than to the depth of the potential well. Simple models in § 6 derive the dependence of mass and metal loss as a function of galaxy rotation speed. Following the conclusions in § 7, Appendix A presents a proof showing how the effective yields calculated for simple "impulsive" gas flows are limiting cases of those that result from arbitrary chemical evolution histories. Appendix B reexamines the conclusions of the paper using the smaller sample of abundances calculated by Garnett (2002).

[3] Note that there is no plausible process that can increase the effective yield, as proved by Edmunds (1990) and shown graphically in an elegant paper by Köppen & Edmunds (1999). The only exception is accretion of metal-rich gas, a highly unlikely possibility that will not be considered further in this paper. Thus, the largest observed value of $y_{\rm eff}$ is a lower limit to the true nucleosynthetic yield.

## 2. OBSERVATIONS OF THE EFFECTIVE YIELD

### 2.1. *The Data*

The analysis in this paper is based on the compilation of effective yields and gas mass fractions from Pilyugin et al. (2004). This data set contains the largest number of spiral and dwarf irregular galaxies with uniformly derived abundances, gas masses, and stellar masses. It is significantly larger than the Garnett (2002) sample, which is analyzed separately in Appendix B, and has more accurate measurements of the gas content than those of Tremonti et al. (2004).

The effective yields in Pilyugin et al. (2004) were calculated using gas-phase oxygen abundances measured from H II region spectroscopy using the "*P* method" developed in Pilyugin (2000, 2001a) to match accurate oxygen abundances on the basis of temperature-sensitive line ratios involving the weak [O III] $\lambda$4363 line (the "$T_e$ method"). The *P* method was used to derive abundances in high-metallicity [$12 + \log({\rm O/H}) > 8.2$] "upper branch" H II regions of spiral galaxies, and it results in systematically lower metallicities than those from the more widely adopted $R_{23}$ method (Pagel et al. 1979). The metallicities of the irregular galaxies compiled in Pilyugin et al. (2004) were derived by Richer & McCall (1995) using the $T_e$ method, or by Pilyugin (2001b) using the *P* method. All metallicities were interpolated from the observed radial metallicity gradients to a common galactocentric radius of $0.4R_{25}$. This fiducial radius will not occur at the same number of disk scale lengths in all galaxies, due to variations in galaxy surface brightness. Since lower mass galaxies have lower surface brightnesses on average, their metallicities will be biased toward smaller radii and higher metallicities than the high-mass galaxies in the Pilyugin et al. (2004) sample.

The gas mass fractions for the Pilyugin et al. (2004) sample were calculated using both the molecular and atomic components measured primarily from single-dish observations, assuming an $N({\rm H_2})/I({\rm CO})$ conversion factor of $1 \times 10^{20}$ cm$^{-2}$ (K km s$^{-1}$)$^{-1}$. I have scaled the data to include an additional correction for the mass in helium that had been neglected in Tables 5 and 7 of Pilyugin et al. (2004). The stellar masses were derived assuming a constant *B*-band stellar mass-to-light ratio of $M/L = 1.5$ for the spiral galaxies and $M/L = 1$ for the irregulars.

### 2.2. *Observed Trends of $y_{\rm eff}$, $f_{\rm gas}$, and $V_c$*

Figure 1 shows the relationships among $y_{\rm eff}$, $f_{\rm gas}$, and $V_c$ for galaxy disks, using data from Tables 5 and 7 of Pilyugin et al. (2004). The left and middle panels show how the effective yield varies with galaxy rotation speed (*left*) and gas mass fraction (*middle*). Spiral disks are plotted as stars (Sbc–Sc) or filled circles (Scd–Sd), and irregular galaxies are plotted as open circles. The right panel shows the relationship between $f_{\rm gas}$ and $V_c$, which will be used in later sections.

The effective yield data in Figure 1 show three main trends. First, the effective yield increases with the dynamical mass of a galaxy, as measured by its rotation speed. As discussed in § 1, this trend is typically interpreted as evidence for larger gas outflows in lower mass galaxies. Second, the effective yield saturates

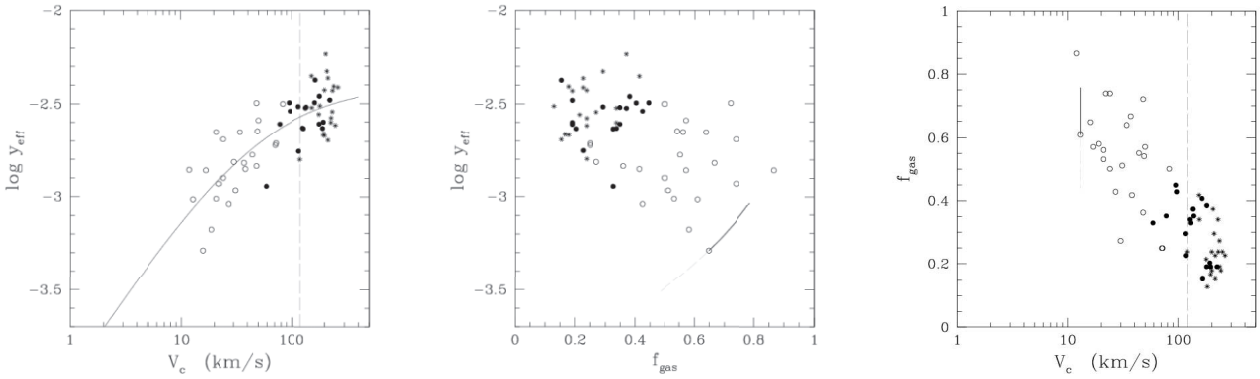


FIG. 1.—Effective yield as a function of galaxy rotation speed (*left*) and of gas mass fraction (*middle*), measured at $0.4R_{25}$ by Pilyugin et al. (2004). The right panel shows the relationship between gas fraction and rotation speed for the same data. Midtype spiral galaxies (Sbc–Sc) are plotted as stars, late-type spirals (Scd–Sd) are plotted as filled circles, and irregulars are plotted as open circles. Compared to massive spirals, the effective yield is reduced by nearly a factor of 10 in low-mass galaxies ($V_c < 40$ km s$^{-1}$), all of which are gas-rich ($f_{gas} > 0.3$). In the left and right panels, the vertical dashed line indicates the rotation speed below which dust lanes disappear and star formation becomes inefficient (Dalcanton et al. 2004; Verde et al. 2002). In the middle and right panels, the short curves show how $y_{eff}$ and $f_{gas}$ would change if the measurement of the gas mass (*dashed line*) or the stellar mass (*solid line*) were reduced by a factor of 2. The solid curve in the left panel shows the fitting formula adopted in § 6. [*See the electronic edition of the Journal for a color version of this figure.*]

at $\log(y_{eff}) \approx -2.4$. I adopt this as the true nucleosynthetic yield (i.e., $y_{true} = 0.004$) throughout this paper.[4] This yield is within the range of theoretical determinations of the oxygen yield (see compilation in Henry et al. 2000 for a Salpeter initial mass function), although it is perhaps on the low side. Third, the galaxies with low effective yields are relatively gas-rich.[5]

### 2.3. *Uncertainties*

One uncertainty in the data shown in Figure 1 is the appropriate value of $f_{gas}$. The equations of chemical evolution track a system in which all of the gas is affected by enrichment. However, the existence of radial abundance gradients (e.g., Zaritsky et al. 1994; van Zee et al. 1998) implies that the entire gas reservoir of a disk galaxy does not necessarily participate equally in the chemical evolution of the system. Thus, the gas that is enriched may only be a fraction of the total gas mass. This discrepancy may be particularly severe for dwarf irregular galaxies, whose H I envelopes extend well beyond their optical radii.

To constrain the impact of the uncertainty in the appropriate gas mass, the dashed curves in the middle and right panels of Figure 1 show the locus of the effective yield and gas mass fraction if the appropriate gas mass is up to a factor of 2 times smaller than assumed. This correction reduces the effective yield, but not significantly. The solid curve is the equivalent locus if the stellar mass has been overestimated by up to a factor of 2, due to uncertainties in the appropriate stellar mass-to-light ratio. In general, these uncertainties are much smaller than the range of $y_{eff}$ and $f_{gas}$ spanned by the data and could not erase the trends seen in Figure 1. The uncertainty in $f_{gas}$ does not affect the metallicity $Z_{gas}$ in equation (2), because the metallicity is determined locally within an H II region through an analysis of emission lines and does not require knowledge of the total gas reservoir.

[4] Models in § 6 find that true yields in the range from $\log(y_{true}) \approx -2.5$ to $-2.3$ also provide statistically equivalent fits to the data.

[5] Note, however, a recent paper by van Zee & Haynes (2006) that finds the opposite trend within a sample of isolated dwarf irregular galaxies. There is currently no satisfactory way to reconcile these two contradictory results. Possible but unattractive solutions are (1) that the behavior seen by van Zee & Haynes (2006) is confined only to dwarf irregular galaxies or (2) that uncertainties in the gas mass fraction are partially responsible, given that errors in $f_{gas}$ scatter points along the observed van Zee & Haynes (2006) relation.

## 3. HOW GAS FLOWS CHANGE THE EFFECTIVE YIELD

If the true nucleosynthetic yield is roughly constant among galaxies, then the observational data in Figure 1 indicate that gas flows must have reduced the effective yield. Before performing detailed calculations, it is useful to explore how gas flows change the effective yield of gas-rich systems, which are the only ones observed with very low effective yields.

First, expanding the definition of the effective yield (eq. [2]) in terms of the gas mass $M_{gas}$, the stellar mass $M_{stars}$, and the mass $M_Z$ in metals in the gas phase gives

$$y_{eff} \equiv \frac{M_Z}{M_{gas}} \frac{1}{\ln\left[\left(M_{gas} + M_{stars}\right)/M_{gas}\right]}. \quad (3)$$

Although $y_{eff}$ was defined on the basis of the closed-box model, it can be calculated for any system, even if $M_{gas}$, $M_{stars}$, and $M_Z$ are not related to each other according to a closed-box model. Equation (3) therefore holds for any past star formation and gas accretion/outflow history.

When the gas mass is much larger than the stellar mass, as seen in low-mass late-type galaxies with low effective yields, a Taylor series expansion of equation (3) yields

$$y_{eff} \approx \frac{M_Z}{M_{stars}}. \quad (4)$$

At high gas mass fractions, the effective yield is therefore independent of how much gas is in the system. This result immediately suggests that accreting even large amounts of gas will make little change in the effective yield of a system that is already gas-rich. Although the additional gas will indeed lower the metallicity of the system (assuming the new gas is metal-poor), it will also increase the gas richness and thus will keep the system near the relationship between $Z_{gas}$ and $f_{gas}$ that is expected for a closed-box system.

Equation (4) also suggests that metal-rich outflows will have a significant impact on the effective yield in gas-rich systems. The effective yield is linear with the mass of metals in the gas phase for a gas-rich system, and thus any process that removes metals leads to an immediate drop in the effective yield.

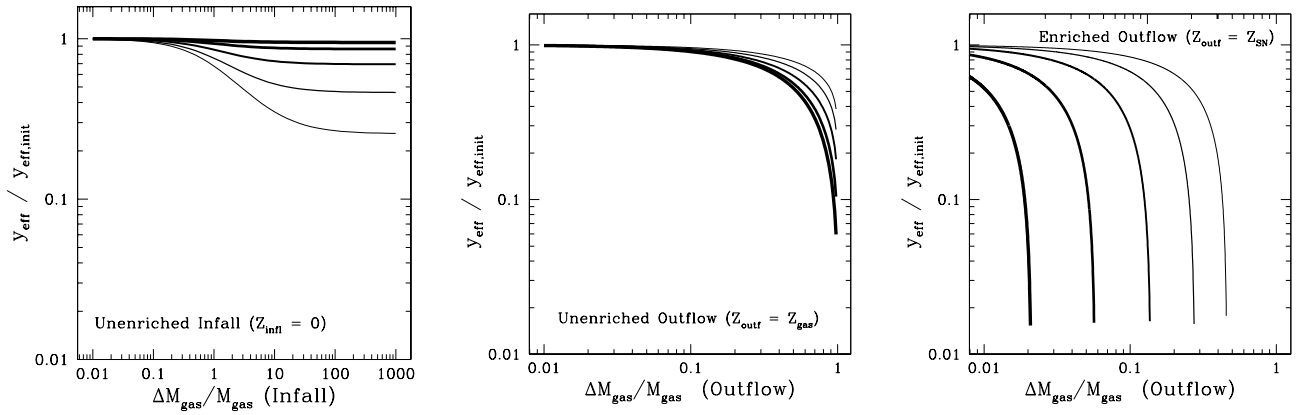


FIG. 2.—Ratio of final to initial effective yield as a function of the ratio of the fractional change in gas mass, $\Delta M_{\rm gas}/M_{\rm gas,\,init}$, for unenriched infall (*left*; $Z_{\rm infl} = 0$), unenriched outflow (*middle*; $Z_{\rm outf} = Z_{\rm gas}$), and enriched outflow (*right*; $Z_{\rm outf} = Z_{\rm SN}$). The solid lines show different initial gas mass fractions ($f_{\rm gas,\,init} = 0.1$, 0.25, 0.5, 0.75, and 0.9, plotted from thin to thick, respectively, which is from bottom to top in the left panel, and from top to bottom in the middle and right panels). With infall, the effective yield is suppressed when large amounts of gas are accreted onto galaxies with low initial gas mass fractions. In the two outflow cases, the effective yield is reduced by large outflows from galaxies with higher initial gas mass fractions. For unenriched outflows, a factor-of-10 decrease in $y_{\rm eff}$ can only be achieved with nearly total gas ablation from initially gas-rich systems. For enriched outflows with large initial gas mass fractions, only modest amounts of enriched outflow are required to produce the factor-of-10 drop in the effective yield seen in Fig. 1.

The gas-rich limit explored above agrees with the more detailed calculations below. Both show that the response of $y_{\rm eff}$ to gas flows is generally insensitive to both inflows (§ 3.1) and unenriched outflows (§ 3.2), but is extremely sensitive to metal-rich outflows (§ 3.2).

### 3.1. *The Response of $y_{\rm eff}$ to Infall*

First consider the extreme case in which gas is added to a system, but no additional stars or metals are formed in response. This scenario produces the maximum possible decrease in the effective yield for a given amount of accretion, as shown in Appendix A, assuming the same initial and final gas mass fractions. If a system starts with an initial effective yield $y_{\rm eff,\,init}$, gas fraction $f_{\rm gas,\,init}$, gas mass $M_{\rm gas}$, and metallicity $Z_{\rm gas}$, and then accretes $\Delta M_{\rm gas}$ of gas with metallicity $Z_{\rm infl}$, the effective yield observed immediately after gas accretion is

$$\frac{y_{\rm eff}}{y_{\rm eff,\,init}} = \frac{1+\left(\Delta M_{\rm gas}/M_{\rm gas}\right)\left(Z_{\rm infl}/Z_{\rm gas}\right)}{1+\left(\Delta M_{\rm gas}/M_{\rm gas}\right)}\,\frac{\ln\left(f_{\rm gas,\,init}\right)}{\ln\left(f_{\rm gas,\,fin}\right)}, \quad (5)$$

and the gas mass fraction is

$$f_{\rm gas,\,fin} = f_{\rm gas,\,init}\,\frac{1+\Delta M_{\rm gas}/M_{\rm gas}}{1+f_{\rm gas,\,init}\left(\Delta M_{\rm gas}/M_{\rm gas}\right)}. \quad (6)$$

The ratio of the final to initial effective yield therefore depends only on the initial gas mass fraction $f_{\rm gas,\,init}$, the ratio $\Delta M_{\rm gas}/M_{\rm gas}$ between the mass of accreted gas and the initial gas mass, and the ratio $Z_{\rm infl}/Z_{\rm gas}$ between the metallicity of the infalling gas and that of the initial gas reservoir.

The left panel of Figure 2 shows the ratio $y_{\rm eff}/y_{\rm eff,\,init}$ for several values of the initial gas mass fraction, assuming that $Z_{\rm infl} = 0$. A few clear trends are apparent. First, the effective yield falls as more gas is added to the system. Second, even when a large amount of gas is added, the effective yield does not drop to an arbitrarily low value and instead levels out to a minimum. Finally, the value of the minimum effective yield depends on the initial gas richness, with smaller changes in $y_{\rm eff}$ produced in systems that were initially gas-rich.

For a given initial gas fraction, equation (5) reaches a minimum as $\Delta M_{\rm gas}/M_{\rm gas} \rightarrow \infty$ when $Z_{\rm infl} = 0$. In this limit, the ratio of the minimum to the initial effective yield becomes

$$\left.\frac{y_{\rm eff}}{y_{\rm eff,\,init}}\right|_{\rm min} = \ln\left(1/f_{\rm gas,\,init}\right)\frac{f_{\rm gas,\,init}}{1-f_{\rm gas,\,init}}. \quad (7)$$

This limit uses the fact that $1+\Delta M_{\rm gas}/M_{\rm gas} = (f_{\rm gas,\,fin}/f_{\rm gas,\,init}) \times (1-f_{\rm gas,\,init})(1-f_{\rm gas,\,fin})^{-1}$ and is plotted in Figure 3 as a function of $f_{\rm gas,\,init}$. As expected from Figure 2, the effective yield can only be suppressed by $\sim$30%–50% for the most gas-rich galaxies ($f_{\rm gas} \sim 0.6$; e.g., West 2005).

The response of a galaxy to gas inflow as a function of the initial gas richness is shown in the left panel of Figure 4, assuming an initial effective yield of $y_{\rm eff} = y_{\rm true}$. Each solid line shows the increase in gas richness and the decrease in effective yield expected for an instantaneous doubling of a galaxy's gas mass due to accretion of metal-free gas. As expected, the drop in effective yield is largest for the most gas-poor galaxies. However, in no case is the drop in effective yield greater than 60%, even for the rather extreme gas accretion shown. In contrast, the data in Figure 1 show nearly a factor-of-10 range of effective yields, which immediately suggests that infall alone cannot be responsible for the low effective yields that are observed. Section 4 discusses this comparison in more detail.

### 3.2. *The Response of $y_{\rm eff}$ to Outflow*

To calculate the response of the effective yield to outflow, consider an "impulsive" gas loss event; that is, one that is not interleaved with any star formation or gas accretion, similar to the infall case considered in § 3.1. This case is a close analog to what might be expected for a wind driven by a cluster of Type II supernovae that followed a burst of star formation; for details of the wind mechanism, see recent reviews by Veilleux et al. (2005) and Martin (2004). As shown in Appendix A, the effective yield immediately following an impulsive outflow will always be larger than the effective yield that would result from a more general, continuous outflow driven by ongoing star formation, assuming that both cases have the same initial and final gas mass fractions and the same mass in the outflow.

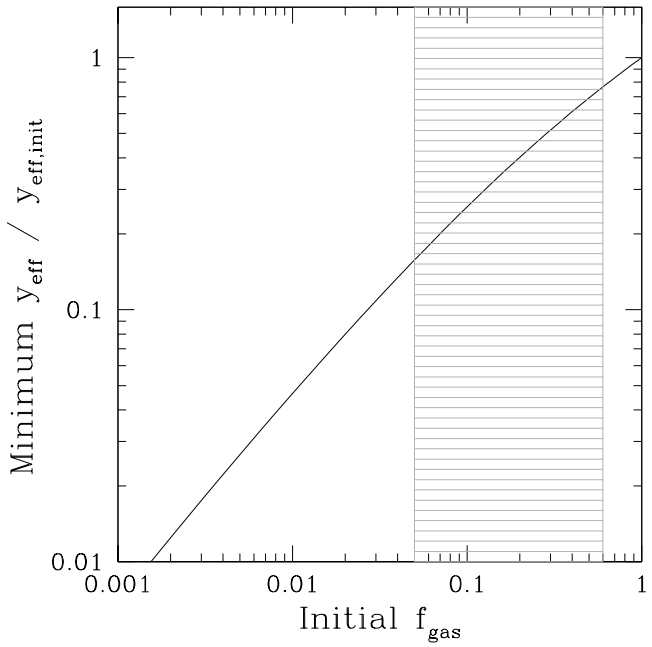


FIG. 3.—Minimum possible effective yield that can be produced by gas accretion, as a function of the initial gas mass of the system. The shaded region indicates the range of gas fractions seen in H I–selected galaxies from the HIPASS survey (West 2005). [*See the electronic edition of the Journal for a color version of this figure*.]

To calculate the impulsive outflow's impact on the effective yield, first define the mass of gas lost due to outflow as $\Delta M_{\rm gas}$ and the mass of metals lost as $\Delta M_Z$. The metallicity of the outflow $Z_{\rm outf}$ is then

$$Z_{\rm outf} = \frac{\Delta M_Z}{\Delta M_{\rm gas}}. \tag{8}$$

The outflow metallicity can be parameterized as a multiple $x$ of the gas phase metallicity at the time of outflow,

$$x \equiv Z_{\rm outf}/Z_{\rm gas}. \tag{9}$$

The maximum value of $x$ is $x_{\rm max} = M_{\rm gas}/\Delta M_{\rm gas}$, which corresponds to a complete loss of metals ($\Delta M_Z = M_Z$).

The ratio $x$ can be constrained observationally using X-ray spectroscopy of hot gas above the midplane of starburst galaxies combined with abundance analyses of H II region emission lines. However, $x$ can also be linked to theoretically motivated quantities by expressing it in terms of the mass fraction of the wind that is entrained gas from the interstellar medium (ISM). In terms of this entrainment fraction $\epsilon$,

$$x = \epsilon + \frac{Z_{\rm SN}}{Z_{\rm gas}}(1-\epsilon), \tag{10}$$

where the metallicity of the supernova ejecta is $Z_{\rm SN}$. The entrainment fraction can be also expressed in terms of the more common "mass loading factor" $\chi$ as $\epsilon = \chi(\chi+1)^{-1}$.

With the above definitions, the effective yield of a galaxy with initial effective yield $y_{\rm eff,\,init}$ and gas mass fraction $f_{\rm gas,\,init}$ becomes

$$\frac{y_{\rm eff}}{y_{\rm eff,\,init}} = \frac{1 - x\Delta M_{\rm gas}/M_{\rm gas}}{1 - \Delta M_{\rm gas}/M_{\rm gas}} \frac{\ln\left(f_{\rm gas,\,init}\right)}{\ln\left(f_{\rm gas,\,fin}\right)} \tag{11}$$

immediately after outflow, where the final gas mass fraction $f_{\rm gas,\,fin}$ is

$$f_{\rm gas,\,fin} = f_{\rm gas,\,init}\frac{1 - \Delta M_{\rm gas}/M_{\rm gas}}{1 - f_{\rm gas,\,init}\Delta M_{\rm gas}/M_{\rm gas}}. \tag{12}$$

The ratio of the final to initial effective yield therefore depends on the initial gas mass fraction $f_{\rm gas,\,init}$, the fraction $\Delta M_{\rm gas}/M_{\rm gas}$ of the initial gas mass lost to outflow, and the ratio $x$ of the metallicity of the outflow to the initial metallicity of the gas.

### 3.2.1. *The Value of x for Realistic Outflows*

Although $x$ can in principle take any value, there are two cases that bracket most realistic supernova- or active galactic nucleus–driven outflows. In the first, the gas in the outflow is dominated by material originally surrounding the supernovae that was driven out after acceleration by shocks. This "blast wave" outflow will have the metallicity of the current ISM, and $x \approx 1$ (corresponding to an entrainment factor of $\epsilon \approx 1$). I refer to this as

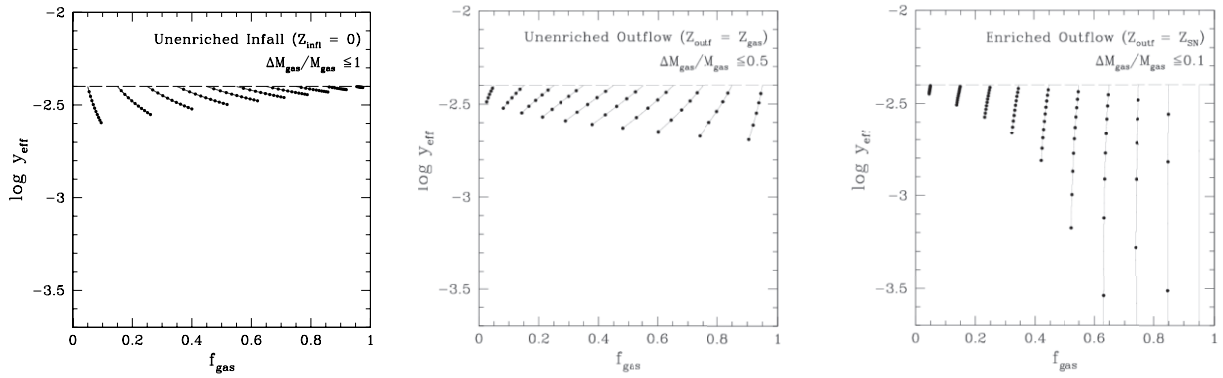


FIG. 4.—Evolution of a galaxy's effective yield and gas mass fraction in response to unenriched infall ($Z_{\rm infl} = 0$; *left*), unenriched outflow ($Z_{\rm outf} = Z_{\rm gas}$; *middle*), and enriched outflow ($Z_{\rm outf} = Z_{\rm SN}$) for different initial gas mass fractions. Each galaxy initially evolves as a closed box with $y_{\rm eff} = y_{\rm true}$, indicated by a horizontal dashed line. Solid lines track the evolution of the effective yield and gas mass fraction when the initial gas mass is doubled by gas accretion (*left*), halved through blast wave outflow (*middle*), or reduced by 10% through enriched outflows (*right*). Dots indicate intervals of $\Delta M_{\rm gas}/M_{\rm gas,\,init} = 0.1$ in the left and middle panels and 0.01 in the right panel. When compared to the middle panel of Fig. 1, neither infall nor unenriched outflows can realistically produce the very low effective yields seen in dwarf irregular galaxies. Simultaneously, the effective yields of more gas-poor, massive disks are insensitive to either gas loss or gas accretion and are unlikely to have effective yields that deviate strongly from the true nucleosynthetic yield, no matter what their evolutionary history. [*See the electronic edition of the Journal for a color version of this figure*.]

the "unenriched outflow" case. For the second class of wind, the material in the outflow is dominated by the ejecta from the supernovae driving the wind. In this scenario, the outflow will be enriched compared to the typical ISM, and $x \geq 1$; I refer to this as the "enriched outflow" case.

To derive the value of $x$ for enriched outflows, I first parameterize the metallicity $Z_{\rm SN}$ of the SN ejecta as a multiple $\eta$ of the nucleosynthetic yield:

$$Z_{\rm SN} = \frac{M_{Z,\,\rm SN}}{M_{\rm ej}} \equiv \eta y_{\rm true}, \tag{13}$$

where $M_{Z,\,\rm SN}$ and $M_{\rm ej}$ are the masses in metals and in gas, respectively, of the SN ejecta. Using the definition of the effective yield ($y_{\rm true} \equiv M_{Z,\,\rm fresh}/M_{\rm remn}$),

$$\eta \equiv \frac{M_{\rm remn}}{M_{\rm ej}} \frac{1}{f_{\rm fresh}}, \tag{14}$$

where $M_{\rm remn}$ is the mass in long-lived stellar remnants and $f_{\rm fresh} \equiv M_{Z,\,\rm fresh}/M_{Z,\,\rm SN}$ is the fraction of the metals in the ejecta that are freshly produced. For oxygen, SN ejecta are almost always dominated by fresh production, with $f_{\rm fresh} \gtrsim 0.9$ for all but supersolar initial stellar metallicities (e.g., Fig. 2 of Chieffi & Limongi 2004). I therefore assume that $f_{\rm fresh} \approx 1$. Note that if $f_{\rm fresh} \approx 1$, then $\eta \approx (1 - R_{M>1\,M_\odot})/R_{M>8\,M_\odot}$, where $R$ is the returned mass fraction for stars evolving in the specified mass range, assuming that (1) stars with $M < 1\ M_\odot$ are unevolved and are locked up over all timescales of interest, (2) only stars with $M > 8\ M_\odot$ (i.e., those with lifetimes <50 Myr) contribute material to the SN ejecta, and (3) only stars with $M > 8\ M_\odot$ produce oxygen. The value of $\eta$ is therefore insensitive to the details of explosive nucleosynthesis and instead depends almost entirely on the initial mass function (IMF) and on the mass lost in SNe and stellar winds.

I have calculated the value of $\eta$ for a variety of IMFs, using the final remnant masses from Table 10 of Portinari et al. (1998) for massive stars ($M_{\rm init} > 8\ M_\odot$) and from Ferrario et al. (2005) for intermediate-mass stars ($1\ M_\odot < M_{\rm init} < 8\ M_\odot$). The resulting values of $\eta$ are $\eta = 4.5$–$5.2$ for the Kroupa (2001) IMF, $\eta = 6.2$–$7.1$ for the Salpeter (1955) IMF, $\eta = 9.2$–$10.2$ for the Kroupa et al. (1993) IMF, and $\eta = 16.8$–$18.6$ for the Scalo (1986) IMF, assuming stellar metallicities between $z = 0.004$ and 0.02. These variations are driven primarily by differences in the high-mass end of the IMF, as can be seen by considering the simplified case in which all stars with >1 $M_\odot$ are completely disrupted either through stellar winds or SNe. In this case, $\eta \approx f_{\rm mass}(M < 1\ M_\odot)/f_{\rm mass}(M > 8\ M_\odot)$, where $f_{\rm mass}$ is the mass fraction of stars in the specified mass range for a given IMF. This estimate gives values of $\eta$ that are $\sim$30% lower than the full calculation. The fraction of mass in low-mass stars varies by $\sim$15% [$f_{\rm mass}(M < 1\ M_\odot) = 0.57$–$0.67$] for the various IMFs considered, but the mass fraction of high-mass stars varies by a factor of 3 [$f_{\rm mass}(M > 8\ M_\odot) = 0.05$–$0.17$ from the Salpeter to the Kroupa 2001 IMFs, respectively]. The variation in $f_{\rm mass}(M > 8\ M_\odot)$ therefore drives the majority of the variation in $\eta$ among different IMFs, more so than differences in the assumed metallicity or mass-loss model.

Current data tend to favor the shallower top-end slope adopted by Kroupa (2001; see review by Chabrier 2003), and thus I adopt a value of $\eta \approx 5$ for the remainder of this paper. If the true value of $\eta$ is higher, then larger entrainment factors would be needed to match the same outflow metallicity. Note that even with this lower value of $\eta$, the wind will be dominated by freshly produced metals for any reasonable value of $f_{\rm gas}$; only a system with $f_{\rm gas} < \exp(-\eta) = 0.007$ would be sufficiently metal-rich for the returned metals to equal the fresh production, assuming that the stars driving the wind were formed recently (i.e., as for a Type II supernova–driven wind) and have metallicities approximately equal to the current gas-phase metallicity. Thus, $x = \eta y_{\rm true}/Z_{\rm gas}$ will be greater than 1 for all reasonable gas fractions.

#### 3.2.2. *Results for Outflows*

Using equation (11) with the appropriate values of $x$, Figure 2 plots the ratio of final to initial effective yield as a function of the mass fraction of gas lost in the outflow ($\Delta M_{\rm gas}/M_{\rm gas}$) for an unenriched outflow (*middle*) and for a maximally enriched outflow with $\epsilon = 0$ (*right*). For unenriched outflows, there are two main results. First, unenriched outflows are most effective in reducing the effective yield of gas-rich galaxies. This trend is in contrast to infall, which causes the largest reductions in $y_{\rm eff}$ when galaxies are gas-poor. Second, even for the most gas-rich galaxies, reducing the effective yield by a factor of 10 requires nearly complete removal of the ISM. Thus, the effective yield is relatively insensitive to outflows that drive out the existing ISM, except in the most extreme case of large gas losses ($\gtrsim$75%) from very gas-rich systems.

For enriched outflows, the situation is quite different. The effective yield is extremely sensitive to gas loss from gas-rich galaxies and decreases without limit for even modest gas loss ($\lesssim$10%).

The sensitivity of $y_{\rm eff}$ to outflow can also be seen in the middle and right panels of Figure 4 for unenriched and enriched outflows, respectively. For galaxies with an initial effective yield of $y_{\rm eff} = y_{\rm true}$ and a range of initial gas mass fractions, these plots show how outflows reduce both the effective yield and the gas richness. Similar to the infall models shown in the left panel, unenriched outflows produce only modest changes in the effective yield, even when half the gas is lost from the system. In contrast, enriched outflows easily produce dramatic drops in the effective yield, particularly for larger gas mass fractions. Metal-enriched outflows are therefore the only viable mechanism for producing the extremely low effective yields seen in Figure 1. Section 4 will discuss this point in more detail.

### 3.3. *Evolution after Gas Accretion or Gas Loss*

Gas accretion and gas loss are likely to be episodic processes (e.g., Marlowe et al. 1995). Thus, while they may temporarily reduce the effective yield, they will likely be followed by periods of closed-box chemical evolution that alter the effective yield while decreasing the gas mass fraction.

To calculate the impact of any subsequent closed-box evolution, assume that a galaxy has an initial effective yield of

$$y_{\rm eff,\,postf} = \frac{Z_{\rm postf}}{\ln(1/f_{\rm gas,\,postf})} \tag{15}$$

immediately after gas accretion or gas loss. The gas mass fraction before the system returns to closed-box evolution is defined as $f_{\rm gas,\,postf} = M_{\rm gas,\,postf}/(M_{\rm gas,\,postf} + M_{\rm stars,\,postf})$. When the galaxy returns to evolving as a closed box, it will obey the equation for instantaneous recycling of a system with fixed baryonic mass:

$$\frac{dZ_{\rm gas}}{dM_{\rm gas}} = -\frac{y_{\rm true}}{M_{\rm gas}}, \tag{16}$$

which shows that the gas-phase metallicity increases proportionally to the true nucleosynthetic yield as the gas mass decreases.

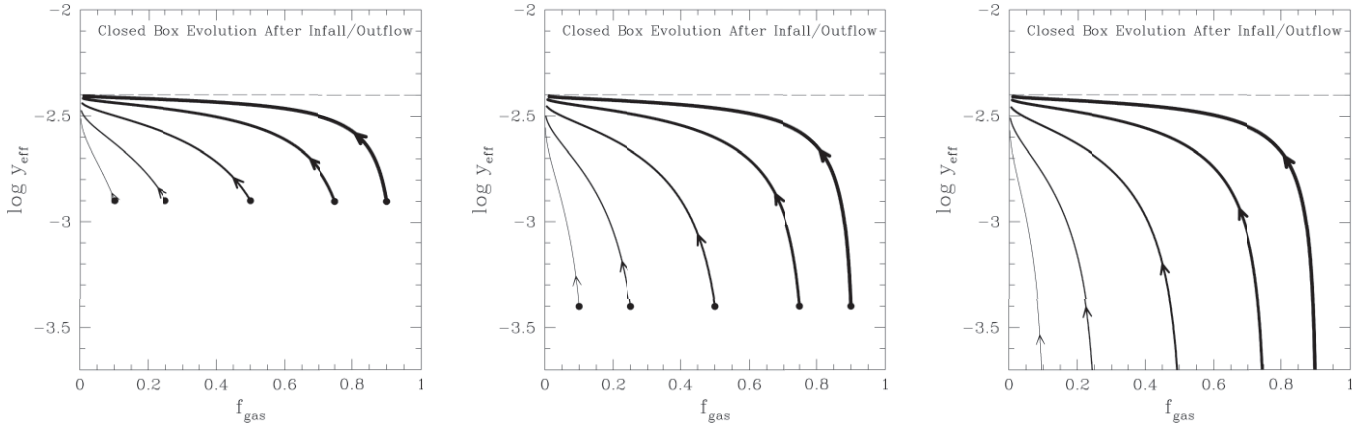


FIG. 5.—Evolution of a galaxy's effective yield and gas mass fraction during closed-box evolution after a temporary reduction in the effective yield, for different initial effective yields ($\log y_{\rm eff,\,postf} = -2.9, -3.4$, and $-3.9$ in the left, middle, and right panels, respectively). In each panel, the different line weights indicate different starting gas mass fractions ($f_{\rm gas,\,postf} = 0.1, 0.3, 0.5, 0.75$, and 0.9, plotted from thin to thick [left to right], respectively). Starting values are marked with filled circles, and arrows indicate the effective yield after the galaxy consumes 10% of its gas. Galaxies evolve from the right to the left of each panel as they convert gas into stars, and they converge to the true nucleosynthetic yield, which is indicated with a dashed horizontal line. For low starting effective yields (*right*), even small reductions in the gas mass fraction cause sharp increases in the effective yield. Thus, low measured effective yields require either frequent enriched outflows or inefficient star formation.

This equation can be integrated using the metallicity and the gas mass immediately after infall/outflow as the initial state:

$$\int_{Z_{\rm postf}}^{Z_{\rm gas}} \frac{dZ_{\rm gas}}{y_{\rm true}} = -\int_{M_{\rm gas,\,postf}}^{M_{\rm gas}} \frac{dM_{\rm gas}}{M_{\rm gas}}, \tag{17}$$

yielding

$$\frac{Z_{\rm gas} - Z_{\rm postf}}{y_{\rm true}} = \ln\left(\frac{M_{\rm gas,\,postf}}{M_{\rm gas}}\right). \tag{18}$$

Equation (18) can be rearranged to solve for $Z_{\rm gas}$ and then substituted into the definition of the effective yield. Using the definition of the effective yield to substitute for $Z_{\rm postf}$ and the fact that $M_{\rm gas} + M_{\rm stars} = M_{\rm gas,\,postf} + M_{\rm stars,\,postf}$ (i.e., no infall or outflow), the effective yield $y_{\rm eff}$ after subsequent closed-box evolution then becomes

$$y_{\rm eff} = y_{\rm true}\left[1 - \frac{\ln(f_{\rm gas,\,postf})}{\ln(f_{\rm gas})}\left(1 - \frac{y_{\rm eff,\,postf}}{y_{\rm true}}\right)\right], \tag{19}$$

where $f_{\rm gas}$ is the gas mass fraction after the system has evolved. Equation (19) shows that when a galaxy returns to closed-box evolution, its effective yield will increase back to the true nucleosynthetic yield as the gas mass fraction decreases. Thus, if star formation is ongoing, the reduction of the effective yield is temporary. This result has also been shown previously by Köppen & Hensler (2005) in a more detailed study of nitrogen and oxygen abundance ratios during episodic infall. The return to closed-box evolution can also be seen in the chemical evolution models of Pilyugin & Ferrini (1998).

To directly track the evolution of the effective yield and gas mass fraction, equation (19) can be rewritten as

$$\frac{y_{\rm eff}}{y_{\rm eff,\,postf}} = 1 + \frac{\ln Q}{\ln(Q f_{\rm gas,\,postf})}\left(\frac{y_{\rm true}}{y_{\rm eff,\,postf}} - 1\right), \tag{20}$$

where $Q \equiv f_{\rm gas}/f_{\rm gas,\,postf}$, a quantity that goes from 1 to 0 as star formation proceeds. Equation (20) shows that the effective yield measured some time after the end of infall/outflow will always increase, by an amount that depends on (1) how low the effective yield was after the flow stopped, (2) how gas-rich the galaxy was, and (3) how much the gas fraction has dropped due to subsequent star formation.

Figure 5 shows the change in $y_{\rm eff}$ and $f_{\rm gas}$ predicted by equation (20) as a function of the initial gas mass fraction (*thin to thick lines*) and the initial postflow effective yield (*left, middle, and right panels*). These curves trace nonintersecting streamlines in the plane of $f_{\rm gas}$ and $y_{\rm eff}$. The curves show the behavior expected from equation (19), namely, that as gas converts into stars and the gas mass fraction decreases, the effective yield rises back toward the true nucleosynthetic yield expected for a closed-box model.

At very low effective yields, the return to closed-box evolution produces a steep fractional rise in the effective yield, due to the linear increase in metallicity with star formation (eq. [16]). Slight decreases in the gas mass fraction due to star formation can therefore drive the effective yield back up to large values. Thus, galaxies will have difficulty maintaining a very low effective yield after infall or outflow has stopped. For example, if a galaxy has an effective yield of $\log y_{\rm eff,\,postf} = -3.5$ and a gas fraction of $f_{\rm gas,\,postf} = 0.5$, then converting just 25% of its gas into stars increases its effective yield by nearly a factor of 10. Figure 5 therefore suggests an additional obstacle to producing a population of galaxies with very low effective yields. These systems must either experience continual infall or outflow, or they must have highly inefficient star formation in order to keep their gas fractions nearly constant and their effective yields low. I return to this point in § 5.

Figure 5 also helps to explain why massive spiral galaxies currently have high effective yields. Spiral disks were probably once gas-rich (Robertson et al. 2006; Springel & Hernquist 2005) and thus must have once been more susceptible to reductions in their effective yields by metal-enriched winds than they are today. Indeed, observations suggest that large-scale outflows were common in massive galaxies at early times (e.g., Adelberger et al. 2003; Steidel et al. 2004; and the recent review by Veilleux et al. 2005), and yet the effective yields of the likely descendants are high. Figure 5 and equation (19) show that any reduction in the effective yield of a gas-rich precursor of a present-day spiral galaxy must be temporary. As the gas-rich disk evolves to its present gas-poor state, its effective yield will rapidly increase back to the nucleosynthetic yield. Thus, the current effective yields of spiral disks place only limited constraints on their past

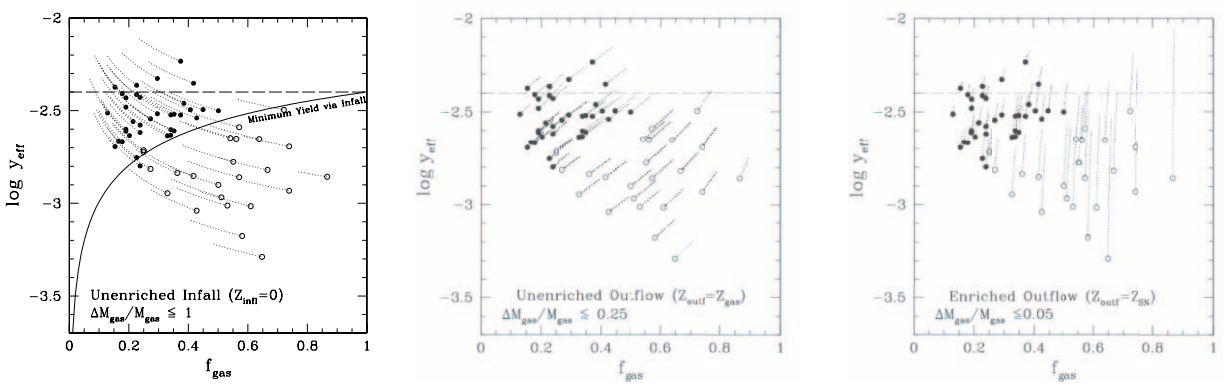


FIG. 6.—Effective yield of spiral ( *filled circles*; Sbc–Sd) and irregular galaxies (*open circles*) as a function of the gas mass fraction for galaxies from Pilyugin et al. (2004). The dotted lines indicate the past effective yield and gas fraction if the present state was produced by doubling the gas mass through accretion (*left*; $Z_{infl} = 0$), by decreasing the gas mass by 25% via unenriched outflows (*middle*; $Z_{outf} = Z_{gas}$), or by decreasing the gas mass by 5% via enriched outflows (*right*; $Z_{outf} = Z_{SN}$). Tracks that do not intersect the horizontal dashed line drawn at the adopted nucleosynthetic yield $y_{true}$ are not likely scenarios for producing the observed data points, or require larger gas flows. Of the three scenarios shown, only enriched outflows are capable of producing the lowest effective yields with realistic gas flows. The effective yields of gas-poor spiral galaxies are insensitive to all outflows, although they can be altered significantly by large amounts of gas accretion. In the left panel, the solid line shows the minimum possible effective yield that infall can produce for systems that begin with a given gas mass fraction, assuming an initial nucleosynthetic yield of $y_{eff,\,init} = y_{true}$. [*See the electronic edition of the Journal for a color version of this figure.*]

gas loss, unless one uses the limiting cases provided in Appendix A. However, in situ measurements of $y_{eff}$ at high redshifts (e.g., Erb et al. 2006) could reveal evidence for an earlier period of outflow. At these redshifts, spiral galaxies are much more likely to be gas-rich and thus will be more likely to show low values of the effective yield for a given amount of outflow.

## 4. CONFRONTING INFALL AND OUTFLOW MODELS WITH DATA

A comparison of the models shown in Figure 4 to the data in the middle panel of Figure 1 immediately suggests that neither gas accretion nor unenriched outflows can reduce effective yields to the low levels seen in low-mass gas-rich dwarf irregular galaxies. Metal-enriched outflows are the only mechanism apparently capable of sufficiently reducing the effective yields. These conclusions are strengthened by factoring in the tendency of postflow evolution to return galaxies to the true nucleosynthetic yield. I now compare each of the three gas flow models with the data in more detail. Appendix B contains an identical comparison with the earlier data from Garnett (2002), reaching similar conclusions.

### 4.1. *Infall Models*

The calculations presented in § 3.1 show that there is an absolute minimum value of the effective yield that can be produced by gas accretion (eq. [7]; Fig. 3). Gas-rich galaxies have the largest value of this minimum, making their effective yields essentially impossible to change by gas accretion. The existence of gas-rich galaxies with low effective yields therefore immediately proves that infall alone cannot produce the necessary reduction in $y_{eff}$.

To show this limit, the left panel of Figure 6 reproduces the data points from Figure 1, with the minimum effective yield that can be reached via infall (eq. [7]) at each gas fraction, assuming an initial effective yield of $y_{eff} = y_{true}$, superimposed. Clearly, all of the irregular galaxies and a few of the spirals (NGC 598, NGC 925, and NGC 2403) have effective yields that are too low to be explained solely by infall. Thus, outflows must have occurred during these galaxies' evolution.

To demonstrate the limits of infall more clearly, the dotted lines in Figure 6 indicate how past gas accretion could have brought galaxies to their present values of $y_{eff}$ and $f_{gas}$. These loci are based on the rather extreme assumption that the galaxies' gas masses have doubled and that the galaxies are being observed immediately after accretion, before any star formation has taken place. Along the dotted lines, the effective yield drops and the gas mass fraction increases as gas is added to a galaxy, moving the galaxy down to lower effective yields and rightward toward higher gas mass fractions. However, even with these generous assumptions, none of these galaxies' loci intercept the horizontal dashed line that indicates the value expected for closed-box evolution. Thus, before the hypothetical gas accretion, some other process would have needed to suppress the galaxies' effective yields below the expected closed-box value. Infall alone is therefore incapable of producing the lowest effective yields.

The only conceivable way that infall could produce gas-rich galaxies with effective yields below the minimum predicted by equation (7) is if the initial gas mass fraction were low and the amount of accreted gas large. However, the data suggest that this possibility is highly unlikely, given that the required initial gas fractions are much lower than those seen in any disk galaxy. For example, for infall to produce galaxies with $\log y_{eff} = -3.0$, the galaxies initially must have had $f_{gas} < 0.025$, which is typical of gas fractions in elliptical galaxies, not disks. Moreover, a galaxy with such a low initial gas mass fraction would have a very high stellar metallicity, which conflicts with the low stellar metallicities derived for dwarf galaxies using broadband colors and resolved stellar populations (e.g., MacArthur et al. 2004; Skillman et al. 2003; Bell & de Jong 2000; Holtzman et al. 2000; van Zee et al. 1997a); this would also lead to a large metallicity difference between the gas phase and the stars (although see Venn et al. 2003 and Lee et al. 2005 for a possible example of such an offset in the dwarf galaxy WLM). Finally, the necessary accretion would have to be extremely large. For accretion to bring a galaxy with an initial gas fraction of $f_{gas} < 0.025$ up to a final gas fraction of $f_{gas} = 0.5$, the galaxy's gas mass would have to increase by a factor of nearly 20, and its baryonic mass would have to double. However, even this large amount of accretion would not lower the effective yield by the factor of 10 needed to explain the lowest mass galaxies. Infall onto a gas-poor system is also unlikely to produce low effective yields in disks that "regrow" around gas-poor bulges, although they do meet the condition for significant

gas accretion onto gas-poor systems; subsequent star formation in the gaseous disk would have wiped out any temporary reduction in the effective yield, as shown in § 3.3.

Although the comparisons in Figure 6 prove that infall alone is not responsible for low effective yields, they do not necessarily imply that infall has not occurred. Instead, the opposite is true. Because the effective yield is insensitive to infall, gas accretion leaves little trace on the effective yield, particularly for gas-rich galaxies. The effective yields of gas-poor galaxies are potentially more sensitive to past infall (e.g., see the evolution loci in the upper left of the left panel in Fig. 6). However, the spiral galaxies that dominate the gas-poor population of disks are also observed to have high star formation efficiencies (e.g., Kennicutt 1998) and thus should rapidly consume any accreted gas, driving their effective yields back up toward the nucleosynthetic yield (Fig. 5). The effective yields of both gas-rich and gas-poor disk galaxies are therefore unlikely to show *any* sign of past infall, even if it has occurred.

Given that infall has been largely overlooked in recent years due to the pervasive theoretical focus on outflows, it is worth reiterating that the evidence for significant sustained infall onto disk galaxies is substantial and that infall of $\sim 1\ M_{\odot}\ \mathrm{pc}^{-2}\ \mathrm{Gyr}^{-1}$ onto high-mass galaxies is required (1) to solve the G dwarf (van den Bergh 1962; Schmidt 1963) and K dwarf problems (Favata et al. 1997; Rocha-Pinto & Maciel 1998; Kotoneva et al. 2002), as originally suggested by Larson (1972), (2) to provide proper relative abundances of different elements and an extended star formation history in the Milky Way (e.g., Chiappini et al. 1997; Boissier & Prantzos 1999; Chang et al. 1999; Chiappini et al. 2001; Alibés et al. 2001; Fenner & Gibson 2003; Casuso & Beckman 2004; and many others), (3) to explain the high deuterium abundances seen in the Milky Way (e.g., Quirk & Tinsley 1973; Chiappini et al. 2002), and (4) to explain the broadband colors, gas fractions, and metallicities of galaxies at low and high redshifts (Boissier & Prantzos 2000; Ferreras et al. 2004). In low-mass galaxies, infall is required to explain why their star formation rates are typically observed to rise to the present day (e.g., Brinchmann et al. 2004; Gavazzi et al. 2002). Such a systematic rise can only occur if the gas surface density is rising with time, as would be expected for gas infall onto a system with inefficient star formation (as dwarf galaxies are observed to have; e.g., van Zee et al. 1997b; van Zee 2001; Hunter & Elmegreen 2004). In total, there is strong ancillary evidence for ongoing gas accretion in both low-mass irregular and high-mass spiral galaxies, but no evidence can come from observations of the effective yield alone.

### 4.2. *Unenriched Outflow Models*

The middle panel of Figure 4 shows that the effective yield is nearly as insensitive to unenriched blast wave outflows as to gas accretion. The only significant difference is that unenriched outflows have the opposite dependence on the initial gas mass fraction, causing larger drops in the effective yield for gas-rich galaxies. Even at high gas mass fractions, however, the decrease in effective yield is still far too small to explain the range of effective yields seen in Figure 1.

The middle panel of Figure 6 shows this limitation clearly. The dotted lines show how the galaxies analyzed by Pilyugin et al. (2004) could have arrived at their present gas mass fractions and effective yields by losing 25% of their ISM in an outflow, in the optimistic case that all galaxies were observed immediately after outflow ceased, but before subsequent star formation drove their effective yields back to larger values. If a locus intercepts the horizontal line at the adopted initial yield of $y_{\mathrm{true}}$, then it is possible that unenriched outflows could have brought the galaxy off the expected closed-box evolution to its present position. However, even with these generous assumptions, it is clear that all but one of the dwarf irregular galaxies could not have had a closed-box effective yield before the hypothetical outflow started and that some other process must have already reduced the effective yield.

The middle panel of Figure 6 shows that the effective yields of massive spiral galaxies are also unlikely to have been significantly altered by unenriched outflows. This result is not surprising, given the weaker response of the effective yield to outflow from gas-poor systems.

As with the infall case discussed above, the data in Figure 6 should not be interpreted as evidence against unenriched outflows. Indeed, the calculations in this paper suggest that a large fraction of a galaxy's ISM can be removed without significantly decreasing the galaxy's effective yield. Instead, the data should be interpreted as evidence that unenriched outflows alone cannot be the cause of the low effective yields seen in low-mass galaxies.

### 4.3. *Enriched Outflow Models*

Having ruled out infall and unenriched outflow in §§ 4.1 and 4.2, respectively, the only possible mechanism that can significantly lower the effective yield is metal-enriched outflow, such as would be caused by direct escape of SN ejecta. The models in Figure 4 show that the effective yields of gas-rich galaxies are extremely sensitive to even modest amounts of gas loss, provided that the ejected gas is metal-rich. An enriched outflow that removes less than a fifth of a galaxy's gas can lower the effective yield by more than a factor of 10, provided that more than half of the galaxy's baryonic mass is gaseous.

The right panel of Figure 6 directly compares enriched outflow models (eq. [11]) with the data. As in the other panels, the dotted lines trace how the galaxies could have reached their present position after driving a metal-enriched wind that expelled $\lesssim 5\%$ of the galaxies' gas. Unlike the other panels, however, the majority of the dotted lines intersect the closed-box effective yield, indicating that a modest amount of enriched outflow could have brought the galaxies' effective yields from the true nucleosynthetic yield down to their present low values. Moreover, because the outflow models calculated in § 3.2 give lower limits to the amount of reduction produced by more continuous outflows, it is possible that even weaker winds may be sufficient to produce the same reduction in $y_{\mathrm{eff}}$ (for example, if the wind began when the galaxies had higher gas fractions and then was followed by or interleaved with star formation).

Taken together, the various panels in Figures 4 and 6 explain why there are few gas-poor galaxies with low effective yields. There are simply no viable scenarios capable of producing such systems. Indeed, all three mechanisms explored in this paper leave the region with $\log y_{\mathrm{eff}} \lesssim -2.8$ and $f_{\mathrm{gas}} \lesssim 0.4$ vacant for any reasonable amount of gas accretion or gas loss.

### 4.4. *Subsequent Evolution Models*

The dotted lines in Figure 6 assume that all galaxies have been observed immediately after infall or outflow. However, given the episodic nature of these processes, it is more likely that most of the galaxies are being observed in a more quiescent state and are turning gas into stars without any significant gas flows. The galaxies are therefore more likely to have recently evolved as a closed box.

To demonstrate how recent closed-box evolution could have brought the galaxies to their current effective yields, Figure 7 shows the data from Pilyugin et al. (2004), along with dotted lines indicating their past effective yields and gas mass fractions,

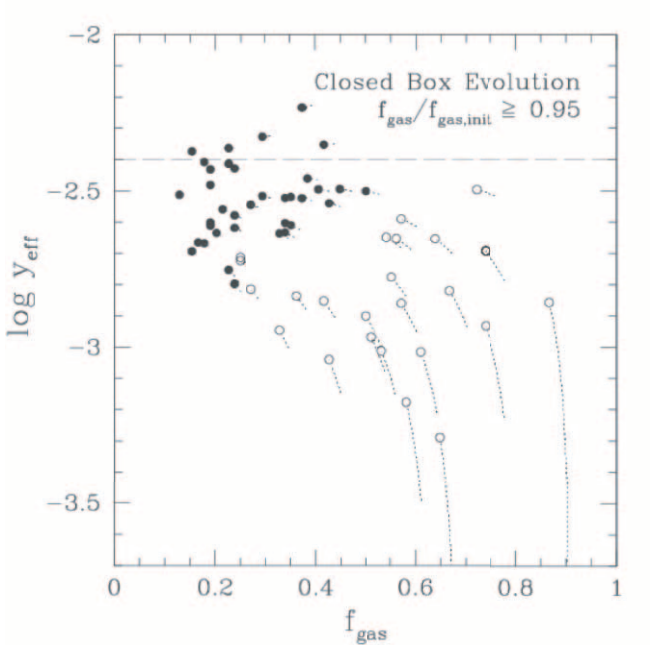


FIG. 7.—Effective yield of spiral (*filled circles*; Sbc–Sd) and irregular galaxies (*open circles*) as a function of the global gas mass fraction for galaxies from Pilyugin et al. (2004). The dotted lines indicate the past effective yield and gas fraction if the present values were produced by closed-box evolution that took place after outflow or infall had stopped. This subsequent evolution reduces the gas mass fraction and pushes the effective yield back to the assumed nucleosynthetic yield, as shown in Fig. 5. The length of the line assumes that the galaxy has converted only 5% its initial gas into stars to reach the present value. Even assuming this very modest evolution, the galaxies with the lowest effective yields and/or largest gas mass fractions would have had substantially lower effective yields in the past. [*See the electronic edition of the Journal for a color version of this figure*.]

assuming that star formation has reduced their initial gas fraction by 5% to reach their present values. As expected from Figure 5, Figure 7 shows that galaxies with low effective yields are extremely sensitive to any subsequent star formation. If such galaxies have recently converted just a small fraction of their gas into stars, then their past effective yields must have been even lower than currently observed. Maintaining low effective yields therefore requires either nearly continuous metal-rich outflows or extremely low star formation rates.

## 5. THE BREAK IN $y_{\rm eff}$ VERSUS $V_c$: OUTFLOWS AND STAR FORMATION EFFICIENCY

### 5.1. *A Mass Threshold for Gas Loss?*

The onset of low effective yields in low-mass galaxies is usually interpreted as evidence for a mass-dependent threshold for mass loss by winds (e.g., Garnett 2002; Tremonti et al. 2004). In these scenarios, the fraction of gas and metals that remain bound to a galaxy is assumed to be a strong function of the depth of the galaxy's gravitational potential well. Low-mass galaxies have shallow potentials and thus should retain only a small fraction of their gas for winds whose energies exceed the depth of the potential. For example, a simple scaling argument presented by Tremonti et al. (2004) suggested that galaxies with circular velocities of less than $V_c \sim 85$ km s$^{-1}$ retain fewer than half of their metals.

In contrast to this widely adopted picture, the results above (and Fig. 4 in particular) suggest that massive galaxies may also have expelled a large fraction of their gas. Although these galaxies are observed to have high effective yields, they are also moderately gas-poor and thus their effective yields can never be significantly reduced by outflows. Massive disk galaxies also have continuous, relatively high rates of star formation, and thus their effective yields rebound quickly from any temporary reduction. Thus, the drop in the effective yield seen in galaxies with $V_c \lesssim 120$ km s$^{-1}$ does not necessarily indicate that *only* these lower mass galaxies have experienced outflows.

If massive galaxies have also driven strong winds, then the trend toward low effective yields is not necessarily due to increasing mass loss. Instead, it can be due to low-mass galaxies' higher gas richness,[6] which increases the sensitivity of the effective yield to mass loss. Thus, even if all galaxies lost the *same* fraction of gas, the effective yield would be lower in dwarf galaxies due to their systematically higher gas fractions. The actual dependence of outflows on galaxy mass is calculated below in § 6, after including variations due to gas richness, and is found to be much weaker than previously assumed.

### 5.2. *Why Is There a Break?*

Given that the gas fraction varies smoothly with rotation speed, why is there an apparent break in the relationship between $y_{\rm eff}$ and $V_c$? Are there plausible mechanisms that could produce a transition at $V_c \sim 120$–$125$ km s$^{-1}$, other than a sharp increase in mass loss? First, inspection of the left panel of Figure 4 shows that $y_{\rm eff}$ responds nonlinearly to the gas mass fraction for a fixed amount of outflow. Small changes in $f_{\rm gas}$ produce much larger changes in $y_{\rm eff}$. Secondly, several groups (Verde et al. 2002; Dalcanton et al. 2004) have noted that below $V_c \sim 120$ km s$^{-1}$, disk galaxies have surface densities that lie entirely below the Kennicutt (1989) threshold for efficient star formation. Their low star formation efficiencies would keep low-mass, low surface density galaxies gas-rich and would allow low effective yields to be maintained after they were established. These two effects could potentially produce a break in the relationship between $y_{\rm eff}$ and $V_c$. By Occam's razor, the coincidence of these two mass scales is strong circumstantial evidence that the variation in star formation efficiency, rather than the depth of the potential well, is critical for producing the transition in the trend of $y_{\rm eff}$ with $V_c$.

Indeed, only a galaxy that falls off the Kennicutt (1998) global Schmidt law can realistically maintain low effective yields between episodes of outflow. To demonstrate the need for low star formation efficiencies, first assume that outflows are discrete events, separated temporally by $\Delta t$. To maintain an effective yield of $\log y_{\rm eff} < -3$ during the interval between outflows, no more than 2.5% of a galaxy's gas ($\Delta f_{\rm gas,\,SF} < 0.025$) must have been converted to stars since the end of the last outflow, setting an upper limit to the star formation rate. For a galaxy that follows the Schmidt law to have a star formation rate less than this upper limit [$<(0.25 \times 10^{-3}\, M_\odot\ {\rm s}^{-1}\ {\rm kpc}^{-2})(\Delta t/10^9\ {\rm yr})^{-1}(\Sigma_{\rm gas}/10\, M_\odot\ {\rm pc}^{-2})$], its current gas surface density must be less than $\Sigma_{\rm gas} < (0.0032\, M_\odot\ {\rm pc}^{-2})(\Delta f_{\rm gas,\,SF}/0.025)^{2.5}(\Delta t/10^9\ {\rm yr})^{-2.5}$, which is several orders of magnitudes below what is typically observed. However, if a galaxy lies entirely below the Kennicutt (1989) star formation threshold, the gas surface density needed to suppress the star formation rate is much more reasonable. I have estimated the star formation law in this regime from Figure 1 of Kennicutt (1998) as $\Sigma_{\rm SFR} \propto \Sigma_{\rm gas}^{12}$, which is drastically steeper than the Schmidt law. Galaxies with $\Sigma_{\rm gas} \lesssim 10\, M_\odot\ {\rm pc}^{-2}$ fall in this low star

[6] A Spearman rank correlation test on the data from Pilyugin et al. (2004) shows that the correlation between $\log V_c$ and $f_{\rm gas}$ is stronger than that between either quantity and $\log y_{\rm eff}$.

formation efficiency regime, and thus only require that $\Sigma_{\rm gas} < (7.5\ M_\odot\ {\rm pc}^{-2})(\Delta f_{\rm gas,\,SF}/0.025)^{0.09}(\Delta t/10^9\ {\rm yr})^{-0.09}$ to maintain low effective yields between outflow events. Almost all late-type and/or low surface brightness dwarf galaxies have gas surface densities below this threshold (Swaters et al. 2002), and thus they should be capable of maintaining low effective yields between episodes of outflow.

### 5.3. *Possible Limitations*

Given the possibility that the drop in star formation efficiency at $V_c \sim 120$ km s$^{-1}$ is responsible for the transition in the effective yield observed by Garnett (2002), it is worthwhile to reexamine several issues. First is the existence of the transition itself. Garnett (2002) based his claim of a transition on a plot of the logarithm of the effective yield against the rotation speed. His Figure 4 showed a flat relationship with rotation speed above $V_c \sim 125$ km s$^{-1}$. However, when the effective yield is plotted against the logarithm of the rotation speed, as in Figures 1 and 9, the evidence for a sharp transition seems much weaker. There is little dynamic range at rotation speeds above $\sim$100 km s$^{-1}$, such that the data can be adequately fitted by a single power law, giving $y_{\rm eff} \approx 0.002(V_c/100\ {\rm km\ s^{-1}})^{0.444}$ for the data in Figure 9. Statistically, however, functions that have a break in the slope (such as a double power law) have lower $\chi^2$ values than expected for the addition of new parameters, which suggests that there is some change in the behavior of $y_{\rm eff}$ from low to high galaxy masses.

The other remaining issue is the relative strength of the effective yield's correlations with gas mass fraction and rotation speed. If the gas fraction is more critical to setting $y_{\rm eff}$ than rotation speed, then $y_{\rm eff}$ should correlate more strongly with $f_{\rm gas}$ than with $V_c$. The data in Figure 1 show a scatter in $\log y_{\rm eff}$ versus $f_{\rm gas}$ that is 45% higher than in the plot of $\log y_{\rm eff}$ versus $\log V_c$, initially suggesting that a galaxy's effective yield might depend more strongly on its mass than on its gas mass fraction. However, the uncertainty in the measurement of $f_{\rm gas}$ is at least 5 times larger than the uncertainty in $V_c$ and produces scatter that is nearly perpendicular to the mean relationship, as can be seen by the solid and dashed lines in the middle and right panels of Figure 1. This effect maximally broadens the relationship between $f_{\rm gas}$ and $y_{\rm eff}$. The resulting higher uncertainties leave open the possibility that the actual trend with gas mass fraction and star formation efficiency is at least as strong as the trend with rotation speed.

## 6. ESTIMATES OF RECENT GAS LOSS

The previous sections suggest that (1) only moderate mass loss of supernova-enriched material is necessary to explain low effective yields, and (2) there is unlikely to be a sharp increase in gas loss below $V_c \sim 100$–$120$ km s$^{-1}$. These points can be demonstrated with a simple model that calculates the outflows needed to explain the observed trends in the effective yield. The model calculates the mass loss needed for a single outflow event to bring galaxies to their present gas mass fraction and effective yield, assuming that they initially followed closed-box evolution. For a fixed entrainment factor, these assumptions give a strict upper bound to the mass loss needed to explain the observed effective yields, as shown in the second lemma of Appendix A; a more realistic extended outflow and star formation history would lead to effective yields lower than those observed for any gas loss greater than that calculated here.

### 6.1. *Assumptions of the Gas-Loss Model*

To estimate the maximum mass lost as a function of galaxy rotation speed, the current gas mass fraction is parameterized as $f_{\rm gas}(V_c) = 1.083$–$0.158 \ln(V_c)$, with $f_{\rm gas}(V_c)$ constrained to lie between 0 and 1. The effective yield is parameterized as

$$y_{\rm eff}(V_c) = y_{\rm true}/[1 + (V_0/V_c)^\alpha]. \quad (21)$$

Values are assigned to the parameters $\alpha$ and $V_0$ using a $\chi^2$ minimization with respect to the data in Figure 1, assuming a value of $\log(y_{\rm true})$ between $-2.6$ and $-2.2$. The $\chi^2$ minima for all values of $\log(y_{\rm true})$ between $-2.5$ and $-2.3$ are statistically equivalent, which gives parameters for equation (21) of $\alpha = 1.2$ and $V_0 = 31$ km s$^{-1}$ for $\log(y_{\rm true}) = -2.5$ and $\alpha = 0.8$ and $V_0 = 80$ km s$^{-1}$ for $\log(y_{\rm true}) = -2.3$. For these values, plots of equation (21) are nearly indistinguishable over the range of rotation speeds where data exist. The best-fit values of $\alpha = 0.9$ and $V_0 = 54$ km s$^{-1}$ for $\log(y_{\rm true}) = -2.4$ are used throughout this section, and for the curved line in the left panel of Figure 1.

The model uses the equations in § 3.2 to derive the rotation speed dependence of the gas loss needed to produce the observed relations for $f_{\rm gas}(V_c)$ and $y_{\rm eff}(V_c)$. The outflow is assumed to consist of $\Delta M_{\rm gas}$ of gas, a fraction $\epsilon$ of which is entrained gas from the ISM, and $1 - \epsilon$ of which is pure supernova ejecta (eq. [10]). *Chandra* observations of dwarf starburst galaxies by Ott et al. (2005) find entrainment fractions of $\epsilon \sim 50\%$–$83\%$, with the majority being less than 65%. Ott et al. (2005) argue that these entrainment factors are probably overestimates of the amount of ISM mixed with the ejecta and that the actual entrainment fractions are thus likely to be smaller.

As in § 3.2, the metallicity of the supernova ejecta is assumed to be $Z_{\rm SN} = \eta y_{\rm true}$, with $\eta = 5$ and $\log(y_{\rm true}) = -2.4$. Larger values of $\eta$ increase the enrichment of the outflow and reduce the amount of outflow needed to remove sufficient metals. Models with higher or lower adopted values of $y_{\rm true}$ produce similar results for low rotation speeds, where the differences between the observed effective yields and $y_{\rm true}$ are large. The models have larger differences at high rotation speeds, where the difference between $\log(y_{\rm true}) = -2.3$ and $\log(y_{\rm true}) = -2.5$ is a large fraction of the difference between the observed effective yields and $y_{\rm true}$. However, the resulting uncertainty in the actual gas and metal loss at large galaxy masses remains less than a factor of 2. Theoretical determinations of $y_{\rm true}$ currently give no help in resolving this issue, given the large spread of published values and the strong dependence on the IMF.

### 6.2. *Results of the Gas-Loss Model*

Figure 8 shows the resulting upper bounds on the fraction of baryons lost (*left*) and of metals lost (*right*) for a series of entrainment fractions from $\epsilon = 0$ to $\epsilon = 1$ (i.e., from pure SN ejecta to pure blast wave outflows). As seen in the left panel, the fraction of the baryons lost rises monotonically toward low disk masses ($V_c > 10$ km s$^{-1}$) but shows no sharp features indicative of a sudden onset of winds. The maximum fraction of baryons lost is never more than 15% for all entrainment factors less than 75% and only reaches values above 50% for unrealistically high entrainment factors ($\epsilon > 94\%$, corresponding to mass loading of nearly a factor of 20). There is also a relatively small range in the baryonic mass fraction lost by disks. The range could be as small as a factor of 2 if $\log(y_{\rm true}) = -2.3$ and is unlikely to be larger than a factor of 6–7 [i.e., if $\log(y_{\rm true}) = -2.5$].

Given the lack of any obvious feature at $V_c \sim 120$ km s$^{-1}$ and the generally modest overall gas loss implied by Figure 8, the idea that winds are dramatically more effective below some threshold in galaxy mass is not compelling. Instead, mass loss from disks seems to be rather modest overall, and only weakly dependent on galaxy mass. These models therefore suggest that

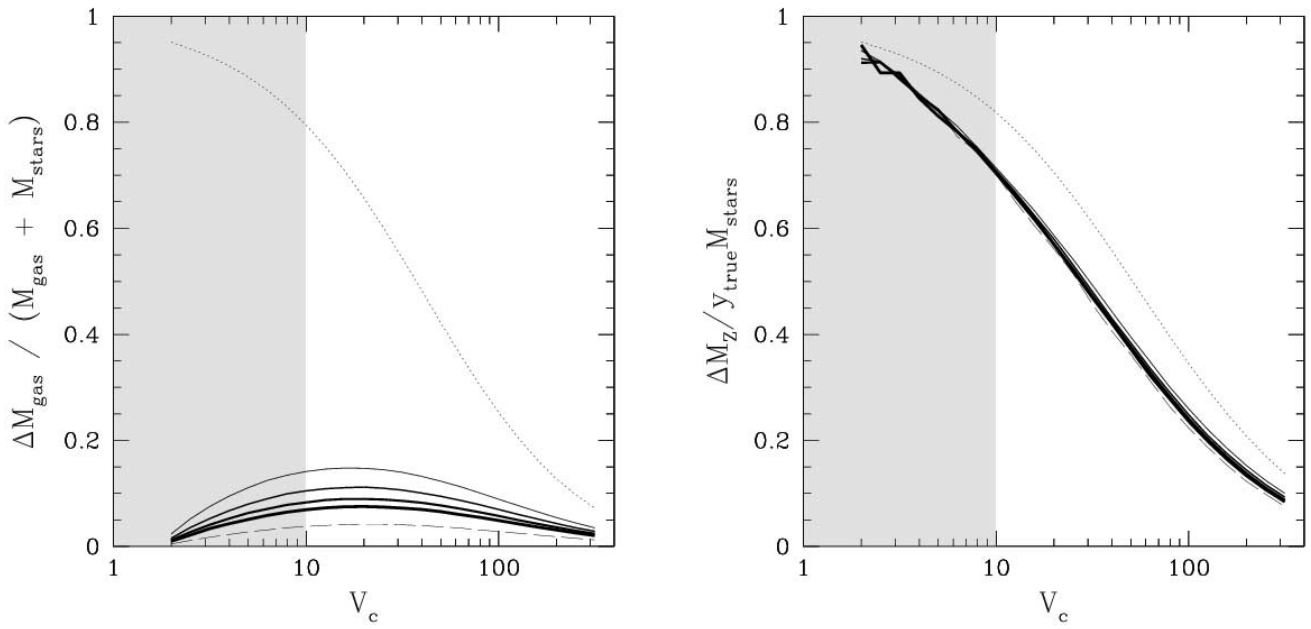


FIG. 8.—Upper limit to the mass fraction of baryons lost (*left*) and metals lost (*right*) as a function of galaxy rotation speed. The lines indicate different fractions of entrained ISM, ranging from 0% (pure SN ejecta; *dashed line*) to 100% (pure blast wave; *dotted line*), with intermediate values of $\epsilon = 0.5-0.8$ in steps of 0.1, plotted as solid lines from thick to thin line weights. The models assume that no infall has taken place and that the galaxies experienced a single outflow event following a period of closed-box evolution. These assumptions guarantee that the mass-loss fractions are the maximum that could be obtained for an arbitrary star formation history involving the same initial and final gaseous and stellar masses. The shaded area indicates the region in which models are unconstrained by current data. [*See the electronic edition of the Journal for a color version of this figure*.]

supernova blowout will not be an effective mechanism for eliminating baryons from low-mass galaxies.

The right panel of Figure 8 shows that the fraction of metals lost is a stronger function of galaxy mass, rising steadily from 10%–25% at $V_c = 200$ km s$^{-1}$ to 50%–60% at ~20–30 km s$^{-1}$, with little dependence on the entrainment fraction. Thus, the fraction of metals varies by less than a factor of 5 over the entire disk galaxy population and shows no sharp features at any particular disk mass.

Even with the larger fraction of metals lost from low-mass galaxies, it is extremely unlikely that dwarf galaxy winds are responsible for enriching the intergalactic medium (IGM). Weighting the curves in Figure 8 by the baryonic mass function of galaxies indicates that the dominant source of metals and gas into the IGM comes from the most massive galaxies, not the dwarfs. Although low-mass galaxies lose a larger fraction of their metals, the difference in gas loss is not sufficiently large to make up for their lower masses overall. Such galaxies simply do not contribute enough to the mass budget of galaxies as a whole to have a significant impact on enrichment of the IGM (see also Calura & Matteucci 2006).

Although Figure 8 confirms that there is some, albeit weak, dependence of outflow strength on galaxy mass, it remains premature to conclude that the physical mechanism driving the correlation is simply the depth of the potential well. There are many galaxy properties that correlate with galaxy mass, and some of these may be more fundamental in limiting the amount of metal loss. The pressure and scale height of the cool ISM and the maximum sizes of H II regions are known to vary with galaxy mass, and all may play some role in determining the structure and efficiency of an outflow. It is also not yet clear if the metals lost from the cool phase are truly lost from the galaxy, rather than kept in a bound hot phase.

Finally, the weak dependence of gas loss on galaxy mass in Figure 8 is indeed a direct result of the correlation between gas mass fraction and rotation speed, as suggested in § 5. If one ignores this dependence and instead assumes a constant gas mass fraction characteristic of spiral galaxies, then galaxies with $V_c \sim 90$ km s$^{-1}$ would have needed to lose nearly twice as much gas as calculated above, and galaxies with $V_c \sim 20$ km s$^{-1}$ would have had to lose more than 90% of their gas. When the variation of gas mass fraction with rotation speed is included, the required mass loss is significantly smaller.

## 7. CONCLUSIONS

This paper has presented a series of calculations showing the impact that inflow (§ 3.1), outflow (§ 3.2), and subsequent closed-box evolution (§ 3.3) have on the effective yield and gas mass fraction of galaxies. These calculations, and their comparison with observations (§ 4–§ 6), yield the following conclusions:

1. There is a minimum effective yield that can be produced by gas accretion. The minimum is significantly higher than the effective yields observed in low-mass galaxies. Thus, low effective yields cannot be due to gas infall.
2. Outflows that drive out gas with the mean metallicity of the ISM can only produce low effective yields if they remove nearly the entire ISM. Because the same galaxies that show low effective yields also show high gas fractions, outflows of unenriched gas cannot produce low effective yields.
3. Outflows that consist primarily of escaped SN ejecta are extremely efficient at reducing the effective yield. Metal-enriched outflow is therefore the only viable mechanism for producing galaxies with low effective yields.
4. Metal-enriched outflows are ineffective at reducing the effective yields of gas-poor systems. Thus, only galaxies that have maintained high gas mass fractions will show depressed effective yields in response to outflow. Only galaxies with inefficient star formation are capable of remaining gas-rich to the

present day, and thus they are the only systems that can show significantly depressed effective yields.

5. Any star formation that takes place after gas accretion or gas loss will increase the effective yield back to the true nucleosynthetic yield expected for closed-box evolution. Thus, only galaxies with inefficient star formation can maintain low effective yields long after infall or outflow has finished.

6. Points 4 and 5 suggest that, in addition to the ability to drive winds, galaxies with low effective yields must also have high gas mass fractions and low star formation rates. Thus, the drop in effective yield observed at $V_c \sim 120$ km s$^{-1}$ ($M_{\rm bary} \sim 10^{10}\ M_\odot$) cannot be interpreted solely as a mass threshold for escape of SN-driven winds. More massive galaxies may have also experienced significant outflows but will show no reduction in their effective yields due to their low gas mass fractions and efficient star formation.

7. Points 1 and 2 should not be taken as evidence that infall and unenriched outflows have not occurred. They only indicate that these two processes produce little noticeable change in a galaxy's effective yield.

8. At high redshifts, a larger fraction of galaxies are likely to be gas-rich. Therefore, a larger fraction of high-redshift galaxies will show reduced effective yields, even if the rates and sizes of typical outflows are identical to those at the present day.

9. The current data on the effective yield and gas mass fraction as a function of galaxy rotation speed suggest that the fraction of metals lost due to outflows increases steadily toward lower mass galaxies, reaching 50% at $\lesssim 30$ km s$^{-1}$. However, the fraction of baryonic mass lost is quite modest ($\lesssim 15\%$) at all galaxy masses. Neither the fraction of metals lost nor the fraction of baryons lost shows a significant feature at $V_c \sim 120$ km s$^{-1}$.

10. If either the initial mass function or the nucleosynthetic yield depends strongly on metallicity, then the amount of gas and metal loss needed to explain the effective yield data would be different than calculated above.

The author gratefully acknowledges discussions with Andrew West, Alyson Brooks, Anil Seth, Crystal Martin, Yong-Zhong Qian, Don Garnett, and Peter Yoachim. A referee also made several suggestions that significantly extended and improved the manuscript. J. J. D. was partially supported through NSF grant CAREER AST 02-38683 and the Alfred P. Sloan Foundation.

## APPENDIX A

## CONTINUOUS VERSUS IMPULSIVE CHEMICAL EVOLUTION

The calculations in this paper consider the impact of single "impulsive" episodes of chemical evolution on the effective yield. However, gas accretion, outflow, and star formation are likely to be continuous and interleaved. In this Appendix, I show that these impulsive cases are strict upper and lower bounds on the effective yield produced by more continuous chemical evolution models. The proof rests on three lemmas (proved in §§ A2–A4) governing how the effective yield changes when swapping the order of two sequential impulsive episodes: (1) star formation followed by gas accretion always produces a lower effective yield than gas accretion followed by star formation; (2) star formation followed by gas outflow always produces a higher effective yield than gas outflow followed by star formation; (3) sequential episodes of gas accretion and gas outflow produce identical effective yields, independent of the order of the two events. Physically, the first lemma is true because gas accretion produces the largest drop in the effective yield of gas-poor systems. Thus, if star formation occurs first, it reduces the gas mass fraction and increases the impact of the infall. Similarly, the second lemma is true because outflows produce the largest drop in the effective yield of gas-rich systems. Thus, the outflow's impact is largest if it occurs before star formation has reduced the gas-richness.

With these lemmas, I show that for the accretion, outflow, and conversion into stars of fixed quantities of gas, the minimum effective yield is produced when impulsive outflow is followed by closed-box star formation and then followed by impulsive gas accretion. The maximum effective yield is produced when the order of these processes is reversed (i.e., infall, followed by star formation, followed by outflow). These extremes allow one to calculate the range of possible effective yields produced by an arbitrary star formation and gas flow history.

### A1. IMPULSIVE CHEMICAL EVOLUTION AS A LIMITING CASE

Assume that during some interval of time $\Delta M_{\rm stars}$ is converted from gas into stars, $\Delta M_{\rm infl}$ of gas is accreted along with $\Delta M_{Z,\,\rm infl}$ in metals, and $\Delta M_{\rm outf}$ and $\Delta M_{Z,\,\rm outf}$ of gas and metals are carried away by outflows. For the most general case, assume that there are no constraints on the rate and timing of when the gas is accreted or expelled, or on the rate and timing of when any new stars are formed, provided that the correct totals are reached at the end of the time interval. Given this freedom, how can the timing of the infall, outflow, and star formation be adjusted to produce the maximum reduction in the effective yield at the end of the time interval?

An arbitrary continuous chemical evolution history can be approximated as an interleaved series of infinitesimal impulsive episodes of star formation, gas infall, and gas outflow, each of which produce changes $\delta M_{{\rm stars},\,i}$, $\delta M_{{\rm infl},\,i}$, $\delta M_{Z,\,{\rm infl},\,i}$, $\delta M_{{\rm outf},\,i}$, and $\delta M_{Z,\,{\rm outf},\,i}$ in the mass of gas, stars, and metals. This time sequence can be represented as

$$\mathbf{I}_1\mathbf{O}_1\mathbf{S}_1\mathbf{I}_2\mathbf{O}_2\mathbf{S}_2\mathbf{I}_3\mathbf{O}_3\mathbf{S}_3\ldots, \tag{A1}$$

where $\mathbf{S}_i$ represents impulsive (closed box) star formation of $\delta M_{{\rm stars},\,i}$ masses of stars, $\mathbf{I}_i$ represents impulsive gas accretion of $\delta M_{{\rm infl},\,i}$ masses of gas along with $\delta M_{Z,\,{\rm infl},\,i}$ masses of metals, and $\mathbf{O}_i$ represents impulsive outflow of $\delta M_{{\rm outf},\,i}$ masses of gas and $\delta M_{Z,\,{\rm outf},\,i}$ masses of metals. These events can be made arbitrarily small so that the sequence closely approximates a continuous chemical evolution history. However, they must obey mass conservation such that $\Delta M_{\rm infl} = \sum_i \delta M_{{\rm infl},\,i}$, $\Delta M_{\rm outf} = \sum_i \delta M_{{\rm outf},\,i}$, and $\Delta M_{\rm stars} = \sum_i \delta M_{{\rm stars},\,i}$.

Now consider reordering pairs in the series above. If some pair is reordered such that it produces a lower effective yield at that point in time, then all subsequent effective yields in the series will be lowered as well, since the final effective yield changes linearly with the initial effective yield (eqs. [5], [11], and [19]). Thus, given some arbitrary star formation and accretion history, one can arrange a lower

final effective yield by reordering any adjacent pair of $\delta M_{\rm infl}$ and $\delta M_{\rm stars}$ so that the gas addition occurs *after* the star formation, or any adjacent pair of $\delta M_{\rm outf}$ and $\delta M_{\rm stars}$ so that the outflow occurs *before* the star formation. Reordering pairs of infall and outflow episodes makes no change in the final effective yield.

Given the lemmas described above (which are proved below), one can make the following reorderings in the series above, switching the terms in brackets in each step:

$$\underbrace{\mathbf{I}_1\mathbf{O}_1}\,\mathbf{S}_1\,\underbrace{\mathbf{I}_2\mathbf{O}_2}\,\mathbf{S}_2\,\underbrace{\mathbf{I}_3\mathbf{O}_3}\,\mathbf{S}_3, \qquad y_{\rm eff,\,1},$$

$$\mathbf{O}_1\,\underbrace{\mathbf{I}_1\mathbf{S}_1}\,\mathbf{O}_2\,\underbrace{\mathbf{I}_2\mathbf{S}_2}\,\mathbf{O}_3\,\underbrace{\mathbf{I}_3\mathbf{S}_3}, \qquad y_{\rm eff,\,2} = y_{\rm eff,\,1},$$

$$\mathbf{O}_1\mathbf{S}_1\,\underbrace{\mathbf{I}_1\mathbf{O}_2}\,\mathbf{S}_2\,\underbrace{\mathbf{I}_2\mathbf{O}_3}\,\mathbf{S}_3\mathbf{I}_3, \qquad y_{\rm eff,\,3} < y_{\rm eff,\,2},$$

$$\mathbf{O}_1\,\underbrace{\mathbf{S}_1\mathbf{O}_2}\,\underbrace{\mathbf{I}_1\mathbf{S}_2}\,\mathbf{O}_3\,\underbrace{\mathbf{I}_2\mathbf{S}_3}\,\mathbf{I}_3, \qquad y_{\rm eff,\,4} = y_{\rm eff,\,3},$$

$$\mathbf{O}_1\mathbf{O}_2\mathbf{S}_1\mathbf{S}_2\,\underbrace{\mathbf{I}_1\mathbf{O}_3}\,\mathbf{S}_3\mathbf{I}_2\mathbf{I}_3, \qquad y_{\rm eff,\,5} < y_{\rm eff,\,4},$$

$$\mathbf{O}_1\mathbf{O}_2\,\underbrace{\mathbf{S}_1\mathbf{S}_2\mathbf{O}_3}\,\underbrace{\mathbf{I}_1\mathbf{S}_3}\,\mathbf{I}_2\mathbf{I}_3, \qquad y_{\rm eff,\,6} = y_{\rm eff,\,5},$$

$$\mathbf{O}_1\mathbf{O}_2\mathbf{O}_3\mathbf{S}_1\mathbf{S}_2\mathbf{S}_3\mathbf{I}_1\mathbf{I}_2\mathbf{I}_3, \qquad y_{\rm eff,\,7} < y_{\rm eff,\,6}.$$

Only in the bottom configuration are there no possible reorderings that could produce a lower effective yield. This final sequence of outflow, followed by closed-box star formation, followed by infall, therefore produces the minimum effective yield of any chemical evolution history that involves the same total gas masses as the first sequence. The above arguments also prove that the minimum effective yield that can be produced by infall of a fixed amount of gas is observed immediately after the infall ceases.

In the same vein, the *maximum* effective yield that can be reached for a given change in the gas and stellar mass can be found by reordering the initial sequence such that each swap produces a *greater* effective yield. The end point of that process is $\mathbf{I}_1\mathbf{I}_2\mathbf{I}_3\mathbf{S}_1\mathbf{S}_2\mathbf{S}_3\mathbf{O}_1\mathbf{O}_2\mathbf{O}_3$. This result also proves that the final effective yield for an arbitrary outflow history is always smaller than if calculated for a single impulsive outflow event.

Taken together, the results above prove that the effective yield produced by an arbitrary continuous chemical evolution history must lie between the two extremes of the impulsive outflow–star formation–inflow case and the impulsive inflow–star formation–outflow case.

The only possible complications in the above proof are if either $\Delta M_{\rm outf} + \Delta M_{\rm stars} > M_{\rm gas,\,init}$ or if $\Delta M_Z > M_{Z,\,\rm init}$ for the minimum effective yield case. If so, there would not be enough gas and/or metals in the initial gas reservoir to support the outflow and subsequent star formation. In these cases, the process of reordering to reach a lower effective yield would be limited by the need to maintain a positive gas mass at all times. However, the same principles apply, and an optimal reordering could be reached for the specific case under consideration.

## A2. INFALL VERSUS CLOSED-BOX STAR FORMATION

To prove that the effective yield is lower if $\delta M_{\rm stars}$ of gas converts into stars before $\delta M_{\rm gas}$ is accreted, consider two cases. In case 1, the gas accretion occurs first and is then followed by closed-box star formation. In case 2, the same events occur in the opposite order. Assume that the initial gas mass fraction and effective yield are $f_{\rm gas}$ and $y_{\rm eff}$, respectively, and that the final gas mass fraction is $f_{{\rm gas},f}$. Assume that the intermediate gas mass fractions (i.e., between the star formation and gas accretion episodes) are $f_{\rm gas,\,1}$ for case 1 and $f_{\rm gas,\,2}$ for case 2. In terms of the initial gas mass fraction,

$$f_{\rm gas,\,1} = f_{\rm gas}\frac{1+Y}{1+Yf_{\rm gas}}, \qquad f_{\rm gas,\,2} = f_{\rm gas}(1-XY), \qquad f_{{\rm gas},f} = f_{\rm gas,\,1}\frac{1+Y-XY}{1+Y}, \tag{A2}$$

where $Y \equiv \delta M_{\rm gas}/M_{\rm gas,\,init}$ (i.e., the fractional change in the gas mass; see eq. [6]) and $X \equiv \delta M_{\rm stars}/\delta M_{\rm gas}$. Also assume that $\Delta Z \equiv \delta M_Z/M_Z$, where $M_Z$ is the initial mass in metals and $\delta M_Z$ is the mass of accreted metals.

For case 1, the intermediate gas mass fraction $f_{\rm gas,\,1}$ can be used in equation (5) to derive the intermediate effective yield after the gas accretion. The intermediate effective yield and gas mass fraction can then be used to calculate the final effective yield $y_{\rm eff,\,1}$ after the subsequent star formation, using a modified form of equation (20):

$$\frac{y_{\rm eff}}{y_{\rm eff,\,postf}} = \frac{\ln f_{\rm gas,\,postf}}{\ln f_{\rm gas}}\left[\left(\frac{\ln f_{\rm gas}}{\ln f_{\rm gas,\,postf}} - 1\right)\frac{y_{\rm true}}{y_{\rm eff,\,postf}} - 1\right]. \tag{A3}$$

If one sets $y_{\rm eff,\,postf}$ and $f_{\rm gas,\,postf}$ to the values after gas accretion, the final effective yield $y_{\rm eff,\,1}$ for case 1 is

$$\frac{y_{\rm eff,\,1}}{y_{\rm eff}} = (1+\Delta Z)\frac{\ln f_{\rm gas}}{\ln f_{{\rm gas},f}}\frac{f_{\rm gas}}{f_{\rm gas,\,1}}\frac{1-f_{\rm gas,\,1}}{1-f_{\rm gas}} \times\left[\left(\frac{\ln f_{{\rm gas},f}}{\ln f_{\rm gas,\,1}} - 1\right)\frac{\ln f_{\rm gas,\,1}}{\ln f_{\rm gas}}\frac{f_{\rm gas,\,1}}{f_{\rm gas}}\frac{1-f_{\rm gas}}{1-f_{\rm gas,\,1}}\frac{1}{1+\Delta Z}\frac{y_{\rm true}}{y_{\rm eff}} - 1\right]. \tag{A4}$$

For case 2, equation (5) and the modified form of equation (20) can be applied in the opposite order as in case 1. The final effective yield $y_{\rm eff,\,2}$ for case 2 is then

$$\frac{y_{\rm eff,\,2}}{y_{\rm eff}} = \left(1 + \Delta Z \frac{M_Z}{M_{Z,\,2}}\right) \frac{\ln f_{\rm gas}}{\ln f_{{\rm gas},f}} \frac{f_{{\rm gas},\,2}}{f_{{\rm gas},f}} \frac{1 - f_{{\rm gas},f}}{1 - f_{{\rm gas},\,2}} \left[\left(\frac{\ln f_{{\rm gas},\,2}}{\ln f_{\rm gas}} - 1\right) \frac{y_{\rm true}}{y_{\rm eff}} - 1\right], \tag{A5}$$

where $M_{Z,\,2}$ is the mass in metals after the initial episode of star formation.

With the above relations, one can compare the final effective yield when the gas accretion occurs first (case 1) to the final effective yield when the gas accretion occurs last (case 2). If one takes the ratio of the final effective yields in the two cases and use the simplifying expressions

$$\frac{\ln f_{{\rm gas},f}}{\ln f_{{\rm gas},\,1}} - 1 = \frac{\ln\left[1 - XY/(1+Y)\right]}{\ln f_{{\rm gas},\,1}}, \qquad \frac{\ln f_{{\rm gas},\,2}}{\ln f_{\rm gas}} - 1 = \frac{\ln\left(1 - XY\right)}{\ln f_{\rm gas}}, \tag{A6}$$

the ratio of the final effective yields of the two cases becomes

$$\begin{aligned}\frac{y_{\rm eff,\,1}}{y_{\rm eff,\,2}} = {} & \frac{1 + \Delta Z}{1 + \Delta Z\left(M_Z/M_{Z,\,2}\right)} \frac{f_{\rm gas} f_{{\rm gas},f}}{f_{{\rm gas},\,1} f_{{\rm gas},\,2}} \frac{(1 - f_{{\rm gas},\,1})(1 - f_{{\rm gas},\,2})}{(1 - f_{\rm gas})(1 - f_{{\rm gas},f})} \\ & \times \frac{1 + \left(A/\ln f_{\rm gas}\right) \ln\left[1 - XY/(1+Y)\right] \left[1/(1+\Delta Z)\right] \left[\left(1 - f_{\rm gas}\right)/f_{\rm gas}\right] \left[f_{{\rm gas},\,1}/\left(1 - f_{{\rm gas},\,1}\right)\right]}{1 + \left(A/\ln f_{\rm gas}\right) \ln\left(1 - XY\right)},\end{aligned} \tag{A7}$$

where $A \equiv y_{\rm true}/y_{\rm eff}$. The third term on the right-hand side is a product of several stellar mass fractions, and is equal to 1. Within the fourth term, $\left[\left(1 - f_{\rm gas}\right)/f_{\rm gas}\right]\left[f_{{\rm gas},\,1}/\left(1 - f_{{\rm gas},\,1}\right)\right]$ simplifies to $1 + Y$, reducing the ratio of $y_{\rm eff,\,1}/y_{\rm eff,\,2}$ to

$$\frac{y_{\rm eff,\,1}}{y_{\rm eff,\,2}} = \frac{1 + \Delta Z}{1 + \Delta Z\left(M_Z/M_{Z,\,2}\right)} \frac{f_{\rm gas} f_{{\rm gas},f}}{f_{{\rm gas},\,1} f_{{\rm gas},\,2}} \frac{1 + \left(A/\ln f_{\rm gas}\right)\left[(1+Y)/(1+\Delta Z)\right] \ln\left[1 - XY/(1+Y)\right]}{1 + \left(A/\ln f_{\rm gas}\right) \ln\left(1 - XY\right)}. \tag{A8}$$

If case 2 indeed produces a lower effective yield than case 1, the ratio of $y_{\rm eff,\,1}/y_{\rm eff,\,2}$ should always be greater than 1. The first term on the right-hand side of equation (A8) is always greater than 1, since the metal mass after star formation $M_{Z,\,2}$ must be greater than the initial mass in metals $M_Z$. The second term is equal to $(1 + Y - XY)/(1 + Y)(1 - XY) = (1 + Y - XY)/(1 + Y - XY - XY^2)$, which is always greater than or equal to 1, due to the additional $-XY^2$ term in the denominator. The third term is always greater than 1 as well, which can be seen by expanding the logarithmic terms as a series:

$$\begin{aligned}\frac{y_{\rm eff,\,1}}{y_{\rm eff,\,2}} = {} & \frac{1 + \Delta Z}{1 + \Delta Z\left(M_Z/M_{Z,\,2}\right)} \frac{f_{\rm gas} f_{{\rm gas},f}}{f_{{\rm gas},\,1} f_{{\rm gas},\,2}} \\ & \times \frac{1 - \left[AXY/\left(\ln 1/f_{\rm gas}\right)\right]\left[1/(1+\Delta Z)\right]\left\{1 + (1/2)\left[XY/(1+Y)\right] + (1/3)\left[(XY)^2/(1+Y)^2\right] + \cdots\right\}}{1 - \left[AXY/\left(\ln 1/f_{\rm gas}\right)\right]\left[1 + (1/2)XY + (1/3)(XY)^2 + \cdots\right]}.\end{aligned} \tag{A9}$$

Since $1 + Y$ is always greater than 1, each term in the series expansion in the numerator is less than or equal to the corresponding term in the expansion in the denominator. Because the prefactor $AXY/\left(\ln 1/f_{\rm gas}\right)$ is always positive and $(1 + \Delta Z)^{-1} < 1$, the numerator of the second term must therefore be greater than the denominator, for any value of the initial effective yield and gas fraction. All three terms on the right-hand side are therefore greater than 1. The product of the three terms must also be greater than 1 as well, thus proving that $y_{\rm eff,\,1}/y_{\rm eff,\,2} > 1$ in all cases, as required to prove that the maximum drop in the effective yield is produced when a system is observed immediately after gas accretion. Physically, accretion has the largest impact on the effective yield when a system is gas-poor. Thus, any star formation that takes place before the infall would reduce the gas-richness, making the infall more effective in reducing the effective yield.

## A3. OUTFLOW VERSUS CLOSED-BOX STAR FORMATION

To prove that the effective yield is higher if $\delta M_{\rm stars}$ of gas converts into stars before $\delta M_{\rm gas}$ and $\delta M_Z$ in gas and metals are expelled, consider two cases. In case 1, the outflow occurs first and is then followed by closed-box star formation. In case 2, the same events occur in the opposite order. If one adopts the same notation as the previous section and assumes that the intermediate gas mass fractions (i.e., between the star formation and outflow episodes) are $f_{{\rm gas},\,1}$ for case 1 and $f_{{\rm gas},\,2}$ for case 2,

$$f_{{\rm gas},\,1} = f_{\rm gas} \frac{1 - Y}{1 - Yf_{\rm gas}}, \qquad f_{{\rm gas},\,2} = f_{\rm gas}(1 - XY), \qquad f_{{\rm gas},f} = f_{{\rm gas},\,1} \frac{1 - Y - XY}{1 - Y}, \tag{A10}$$

where $Y \equiv \delta M_{\rm gas}/M_{\rm gas,\,init}$ (i.e., the fractional change in the gas mass) and $X \equiv \delta M_{\rm stars}/\delta M_{\rm gas}$. Also assume that $\Delta Z \equiv \delta M_Z/M_Z$, where $M_Z$ is the initial mass in metals and $\delta M_Z$ is the mass lost in metals during the outflow. With these definitions, and applying equation (11) (with $\Delta Z$ substituted for $x\Delta M_{\rm gas}/M_{\rm gas}$) and equation (A3),

$$\frac{y_{\rm eff,\,1}}{y_{\rm eff}} = \frac{\ln f_{\rm gas}}{\ln f_{{\rm gas},f}} \frac{1 - \Delta Z}{1 - Y} \left[\left(\frac{\ln f_{{\rm gas},f}}{\ln f_{{\rm gas},\,1}} - 1\right) \frac{\ln f_{{\rm gas},\,1}}{\ln f_{\rm gas}} \frac{1 - Y}{1 - \Delta Z} \frac{y_{\rm true}}{y_{\rm eff}} - 1\right]. \tag{A11}$$

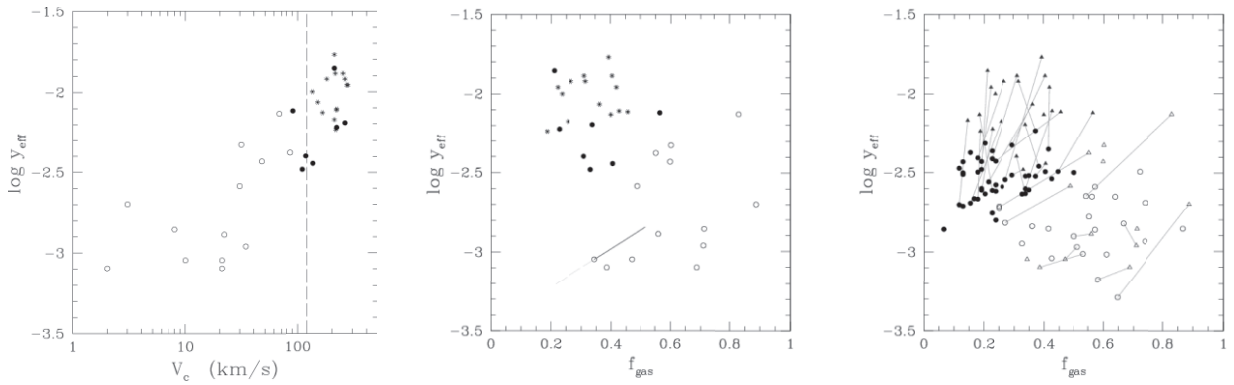


FIG. 9.—Effective yield at the disk half-light radius as a function of galaxy rotation speed (*left*) and gas mass fraction (*middle*), for the data from Table 4 of Garnett (2002). Midtype spiral galaxies (Sbc–Sc) are plotted as stars, late-type spirals (Scd–Sd) are plotted as filled circles, and irregulars are plotted as open circles. Only types Sbc and later are included. All lines in the plots are equivalent to those shown for the Pilyugin et al. (2004) data in the left and middle panels of Fig. 1. The right panel compares the data from Garnett (2002) (*triangles*) to that of Pilyugin et al. (2004) (*circles*), with lines connecting the different measurements reported for identical galaxies. The assumptions used in Garnett (2002) result in larger effective yields and gas mass fractions. See the discussion in Appendix B for the origin of these differences. [*See the electronic edition of the Journal for a color version of this figure*.]

For case 2, equation (11) and equation (A3) can be applied in the opposite order as in case 1. The final effective yield $y_{\rm eff,\,2}$ for case 2 is then

$$\frac{y_{\rm eff,\,2}}{y_{\rm eff}} = \frac{\ln f_{\rm gas}}{\ln f_{{\rm gas},f}} \frac{1-\Delta Z\left(M_Z/M_{Z,\,2}\right)}{1-Y} \left[\left(\frac{\ln f_{\rm gas,\,2}}{\ln f_{\rm gas}} - 1\right)\frac{y_{\rm true}}{y_{\rm eff}} - 1\right], \tag{A12}$$

where $M_{Z,\,2}$ is the mass in metals after star formation, but before outflow, such that $M_{Z,\,2} > M_Z$ in all cases.

With the above relations, one can compare the final effective yield when the outflow occurs first (case 1) to the final effective yield when the outflow occurs last (case 2). If one takes the ratio of the final effective yields in the two cases and use the simplifying expressions

$$\frac{\ln f_{{\rm gas},f}}{\ln f_{\rm gas,\,1}} - 1 = \frac{\ln\{1-[XY/(1-Y)]\}}{\ln f_{\rm gas,\,1}}, \qquad \frac{\ln f_{\rm gas,\,2}}{\ln f_{\rm gas}} - 1 = \frac{\ln(1-XY)}{\ln f_{\rm gas}}, \tag{A13}$$

the ratio of the final effective yields of the two cases becomes

$$\frac{y_{\rm eff,\,1}}{y_{\rm eff,\,2}} = \frac{1-\Delta Z}{1-\Delta Z\left(M_Z/M_{Z,\,2}\right)} \frac{1-\left(A/\ln f_{\rm gas}\right)[(1-Y)/(1-\Delta Z)]\ln[1-XY/(1-Y)]}{1-\left(A/\ln f_{\rm gas}\right)\ln(1-XY)}, \tag{A14}$$

where $A \equiv y_{\rm true}/y_{\rm eff}$.

The first term is always less than 1, because $M_Z/M_{Z,\,2} < 1$. The second term is always less than 1 as well, which can be seen by expanding the logarithmic terms in a series:

$$\frac{y_{\rm eff,\,1}}{y_{\rm eff,\,2}} = \frac{1-\Delta Z}{1-\Delta Z\left(M_Z/M_{Z,\,2}\right)} \frac{1-\left[AXY/\left(\ln 1/f_{\rm gas}\right)\right][1/(1-\Delta Z)]\left\{1+(1/2)[XY/(1-Y)]+(1/3)\left[(XY)^2/(1-Y)^2\right]+\cdots\right\}}{1-\left[AXY/\left(\ln 1/f_{\rm gas}\right)\right]\left[1+(1/2)XY+(1/3)(XY)^2+\cdots\right]}. \tag{A15}$$

Since $1-Y<1$, $\Delta Z<1$, and $AXY/\ln(1/f_{\rm gas})$ is always positive, the second term is always less than 1. The product of the two terms is therefore always less than 1 as well, thus proving that $y_{\rm eff,\,1}/y_{\rm eff,\,2} < 1$ in all cases. Thus, the minimum effective yield is produced when star formation follows outflow. Physically, outflow has the largest impact on the effective yield when a system is gas-rich. Thus, any star formation that takes place before outflow would reduce the gas-richness, making the outflow much less effective in reducing the effective yield.

## A4. INFALL VERSUS OUTFLOW

Assume that there are back-to-back accretion and outflow events. Assume that a mass $\delta M_{\rm infl}$ of gas and $\delta M_{Z,\,\rm infl}$ of metals is accreted and that a mass of $\delta M_{\rm outf}$ of gas and $\delta M_{Z,\,\rm outf}$ of metals is expelled via outflows. Let case 1 be when outflow occurs first, let case 2 be when infall occurs first, and assume the same notation as in previous sections.

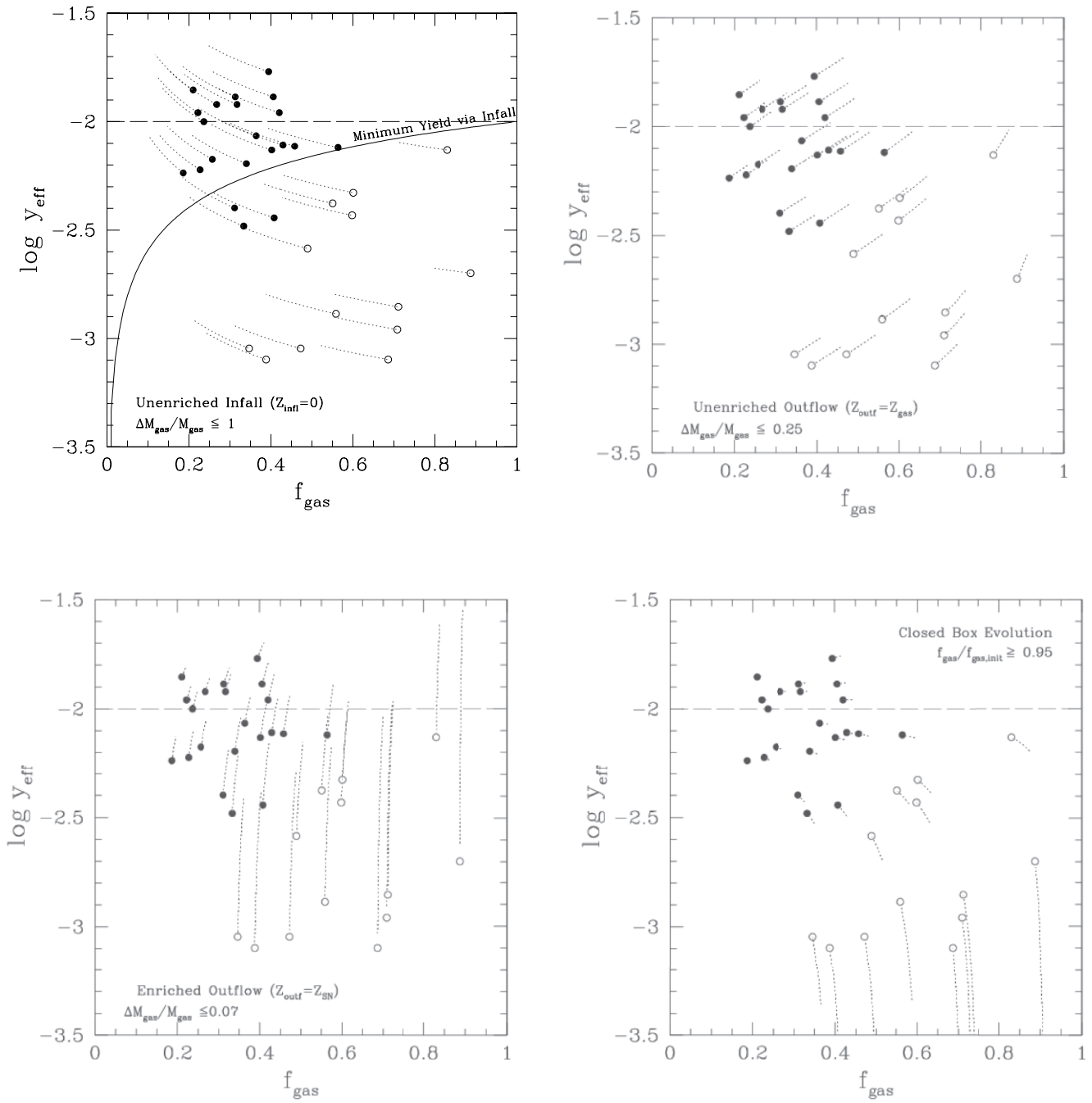


FIG. 10.—Effective yield of spiral (*filled circles*) and irregular galaxies (*open circles*) as a function of the gas mass fraction for galaxies from Garnett (2002). The dotted tracks are equivalent to those in Figs. 6 and 7 for unenriched infall (*top left*), unenriched outflow (*top right*), enriched outflow (*bottom left*), and subsequent closed-box evolution (*bottom right*). [*See the electronic edition of the Journal for a color version of this figure*.]

In case 1 the effective yield after the initial outflow is

$$y_{\mathrm{eff},\,1,\,\mathrm{int}} = \frac{M_Z - \delta M_{Z,\,\mathrm{outf}}}{M_{\mathrm{gas}} - \delta M_{\mathrm{outf}}} \frac{1}{\ln\left[\left(M_{\mathrm{stars}} + M_{\mathrm{gas}} - \delta M_{\mathrm{outf}}\right)/\left(M_{\mathrm{gas}} - \delta M_{\mathrm{outf}}\right)\right]}. \tag{A16}$$

After the subsequent infall, the effective yield becomes

$$y_{\mathrm{eff},\,1} = \frac{M_Z - \delta M_{Z,\,\mathrm{outf}} + \delta M_{Z,\,\mathrm{infl}}}{M_{\mathrm{gas}} - \delta M_{\mathrm{outf}} + \delta M_{\mathrm{infl}}} \frac{1}{\ln\left[\left(M_{\mathrm{stars}} + M_{\mathrm{gas}} - \delta M_{\mathrm{outf}} + \delta M_{\mathrm{infl}}\right)/\left(M_{\mathrm{gas}} - \delta M_{\mathrm{outf}} + \delta M_{\mathrm{infl}}\right)\right]}. \tag{A17}$$

A similar calculation for case 2 yields a different intermediate effective yield, but the final effective yield is identical (i.e., $y_{\mathrm{eff},\,2} = y_{\mathrm{eff},\,1}$). Thus, the order in which infall and outflow occur has no impact on the final effective yield. This symmetry did not occur for the two

previous cases because the fraction of metals locked up by star formation depended on the initial metallicity of the gas, not just on the total mass of gas converted into stars.

## APPENDIX B

## GARNETT DATA

In this section I reproduce the plots from Figures 1, 6, and 7 using the data from the original Garnett (2002) paper rather than that from Pilyugin et al. (2004). Garnett (2002) used the $R_{23}$ technique to derive oxygen abundances and adopted different mass-to-light ratios, $N(H_2)/I(CO)$ conversion factors, and rotation speeds than Pilyugin et al. (2004). Because of the very different metallicity scales adopted by these two papers, the data could not be combined into a single plot in the main body of the paper. These data are included for completeness, but do not substantively change the results of the paper.

Figure 9 shows the effective yield as a function of rotation speed (*left*) and gas mass fraction (*middle*) for the data compiled in Table 4 of Garnett (2002). Like the Pilyugin et al. (2004) sample, the Garnett (2002) sample contains spiral and irregular galaxies drawn from the literature, rectifies all metallicity measurements to a common abundance calibration, and interpolates the resulting metallicities to a common galactocentric radius (the half-light radius for Garnett 2002, versus $0.4R_{25}$ for Pilyugin et al. 2004).

The right panel of Figure 9 shows a direct comparison between the Pilyugin et al. (2004) and Garnett (2002) samples, which have many galaxies in common. Garnett (2002) adopted systematically higher effective yields and higher gas mass fractions. The low effective yields are due primarily to the much higher abundances derived by Garnett (2002), who used the popular $R_{23}$ method (Pagel et al. 1979).

Garnett (2002) also made different assumptions when deriving gas mass fractions. Pilyugin et al. (2004) assumes a constant stellar mass-to-light ratio of $M/L = 1.5$ for spiral galaxies, whereas Garnett (2002) uses a more accurate color-dependent mass-to-light ratio. Both papers adopt a constant stellar mass-to-light ratio of $M/L = 1.0$ for all irregular galaxies. Garnett (2002) also adopts a larger $N(H_2)/I(CO)$ conversion factor and includes a correction for $H_2$ in irregular galaxies that was neglected in Pilyugin et al. (2004), but that has been included in Figure 9. Many of the distances adopted by both papers vary as well, although this affects only the absolute magnitude and not the gas fraction or the effective yield.

Figure 9 suggests a higher true nucleosynthetic yield of $y_{true} = 0.01$, rather than $\log(y_{true}) \approx -2.5$, as adopted throughout the paper. This higher value is in good agreement with theoretical calculations by Maeder (1992) and Nomoto et al. (1997), but slightly higher than the models of Woosley & Weaver (1995), as compiled by Henry et al. (2000) for a Salpeter initial mass function. However, since the results in this paper calculate the ratio of the final to initial effective yield, an overall decrease in the metallicity scale has no effect on our conclusions. On the other hand, because the metallicity calibration adopted by Pilyugin et al. (2004) differs from the $R_{23}$ method primarily at high metallicities, the full range of effective yields in the Pilyugin et al. (2004) sample is a factor of 2 smaller than the range seen in Garnett (2002), reducing the amount of inflow or outflow needed to explain the Pilyugin et al. (2004) data. Figure 10 reproduces the flow models previously applied to Figures 6 and 7 and reaches the same qualitative conclusions. With the larger range of effective yields seen in the Garnett (2002) sample, metal-enriched outflows from gas-rich galaxies are even more necessary to explain the data.

## REFERENCES


Adelberger, K. L., Steidel, C. C., Shapley, A. E., & Pettini, M. 2003, ApJ, 584, 45
Alibés, A., Labay, J., & Canal, R. 2001, A&A, 370, 1103
Bell, E. F., & de Jong, R. S. 2000, MNRAS, 312, 497
Boissier, S., & Prantzos, N. 1999, MNRAS, 307, 857
———. 2000, MNRAS, 312, 398
Brinchmann, J., Charlot, S., White, S. D. M., Tremonti, C., Kauffmann, G., Heckman, T., & Brinkmann, J. 2004, MNRAS, 351, 1151
Calura, F., & Matteucci, F. 2006, MNRAS, 369, 465
Casuso, E., & Beckman, J. E. 2004, A&A, 419, 181
Chabrier, G. 2003, PASP, 115, 763
Chang, R. X., Hou, J. L., Shu, C. G., & Fu, C. Q. 1999, A&A, 350, 38
Chiappini, C., Matteucci, F., & Gratton, R. 1997, ApJ, 477, 765
Chiappini, C., Matteucci, F., & Romano, D. 2001, ApJ, 554, 1044
Chiappini, C., Renda, A., & Matteucci, F. 2002, A&A, 395, 789
Chieffi, A., & Limongi, M. 2004, ApJ, 608, 405
Dalcanton, J. J., Yoachim, P., & Bernstein, R. A. 2004, ApJ, 608, 189
Dekel, A., & Silk, J. 1986, ApJ, 303, 39
Edmunds, M. G. 1990, MNRAS, 246, 678
Erb, D. K., Shapley, A. E., Pettini, M., Steidel, C. C., Reddy, N. A., & Adelberger, K. L. 2006, ApJ, 644, 813
Favata, F., Micela, G., & Sciortino, S. 1997, A&A, 323, 809
Fenner, Y., & Gibson, B. K. 2003, Publ. Astron. Soc. Australia, 20, 189
Ferrario, L., Wickramasinghe, D., Liebert, J., & Williams, K. A. 2005, MNRAS, 361, 1131
Ferreras, I., Silk, J., Böhm, A., & Ziegler, B. 2004, MNRAS, 355, 64
Garnett, D. R. 2002, ApJ, 581, 1019
Gavazzi, G., Bonfanti, C., Sanvito, G., Boselli, A., & Scodeggio, M. 2002, ApJ, 576, 135
Hartwick, F. D. A. 1980, ApJ, 236, 754
Henry, R. B. C., Edmunds, M. G., & Köppen, J. 2000, ApJ, 541, 660
Holtzman, J. A., Smith, G. H., & Grillmair, C. 2000, AJ, 120, 3060
Hunter, D. A., & Elmegreen, B. G. 2004, AJ, 128, 2170
Köppen, J., & Edmunds, M. G. 1999, MNRAS, 306, 317
Köppen, J., & Hensler, G. 2005, A&A, 434, 531
Kennicutt, R. C., Jr. 1989, ApJ, 344, 685
———. 1998, ApJ, 498, 541
Kotoneva, E., Flynn, C., Chiappini, C., & Matteucci, F. 2002, MNRAS, 336, 879
Kroupa, P. 2001, MNRAS, 322, 231
Kroupa, P., Tout, C. A., & Gilmore, G. 1993, MNRAS, 262, 545
Lanfranchi, G. A., & Matteucci, F. 2004, MNRAS, 351, 1338
Larson, R. B. 1972, Nature, 236, 7
———. 1974, MNRAS, 169, 229
Lee, H., Skillman, E. D., & Venn, K. A. 2005, ApJ, 620, 223
MacArthur, L. A., Courteau, S., Bell, E., & Holtzman, J. A. 2004, ApJS, 152, 175
Madau, P., Ferrara, A., & Rees, M. J. 2001, ApJ, 555, 92
Maeder, A. 1992, A&A, 264, 105
Marlowe, A. T., Heckman, T. M., Wyse, R. F. G., & Schommer, R. 1995, ApJ, 438, 563
Martin, C. L. 1998, ApJ, 506, 222
———. 2004, in Origin and Evolution of the Elements, ed. A. McWilliam & M. Rauch (Cambridge: Cambridge Univ. Press), 370
Martin, C. L., Kobulnicky, H. A., & Heckman, T. M. 2002, ApJ, 574, 663
Mori, M., Ferrara, A., & Madau, P. 2002, ApJ, 571, 40
Nomoto, K., Hashimoto, M., Tsujimoto, T., Thielemann, F.-K., Kishimoto, N., Kubo, Y., & Nakasato, N. 1997, Nucl. Phys. A, 616, 79
Ott, J., Walter, F., & Brinks, E. 2005, MNRAS, 358, 1453
Pagel, B. E. J. 1997, Nucleosynthesis and Chemical Evolution of Galaxies (Cambridge: Cambridge Univ. Press)
Pagel, B. E. J., & Edmunds, M. G. 1981, ARA&A, 19, 77
Pagel, B. E. J., Edmunds, M. G., Blackwell, D. E., Chun, M. S., & Smith, G. 1979, MNRAS, 189, 95
Pilyugin, L. S. 2000, A&A, 362, 325
———. 2001a, A&A, 369, 594
———. 2001b, A&A, 374, 412
Pilyugin, L. S., & Ferrini, F. 1998, A&A, 336, 103
Pilyugin, L. S., Vílchez, J. M., & Contini, T. 2004, A&A, 425, 849
Portinari, L., Chiosi, C., & Bressan, A. 1998, A&A, 334, 505
Quirk, W. J., & Tinsley, B. M. 1973, ApJ, 179, 69

Richer, M. G., & McCall, M. L. 1995, ApJ, 445, 642
Robertson, B., Hernquist, L., Bullock, J. S., Cox, T. J., Di Matteo, T., Springel, V., & Yoshida, N. 2006, ApJ, 645, 986
Rocha-Pinto, H. J., & Maciel, W. J. 1998, A&A, 339, 791
Salpeter, E. E. 1955, ApJ, 121, 161
Sandage, A. R. 1965, in The Structure and Evolution of Galaxies (New York: Interscience), 83
Scalo, J. M. 1986, Fundam. Cosmic Phys., 11, 1
Schmidt, M. 1963, ApJ, 137, 758
Searle, L., & Sargent, W. L. W. 1972, ApJ, 173, 25
Silk, J., Wyse, R. F. G., & Shields, G. A. 1987, ApJ, 322, L59
Skillman, E. D., Tolstoy, E., Cole, A. A., Dolphin, A. E., Saha, A., Gallagher, J. S., Dohm-Palmer, R. C., & Mateo, M. 2003, ApJ, 596, 253
Springel, V., & Hernquist, L. 2005, ApJ, 622, L9
Steidel, C. C., Shapley, A. E., Pettini, M., Adelberger, K. L., Erb, D. K., Reddy, N. A., & Hunt, M. P. 2004, ApJ, 604, 534
Swaters, R. A., van Albada, T. S., van der Hulst, J. M., & Sancisi, R. 2002, A&A, 390, 829
Tinsley, B. M. 1980, Fundam. Cosmic Phys., 5, 287
Tremonti, C. A., et al. 2004, ApJ, 613, 898
van den Bergh, S. 1962, AJ, 67, 486
van Zee, L. 2001, AJ, 121, 2003
van Zee, L., & Haynes, M. P. 2006, ApJ, 636, 214
van Zee, L., Haynes, M. P., & Salzer, J. J. 1997a, AJ, 114, 2497
van Zee, L., Haynes, M. P., Salzer, J. J., & Broeils, A. H. 1997b, AJ, 113, 1618
van Zee, L., Salzer, J. J., Haynes, M. P., O'Donoghue, A. A., & Balonek, T. J. 1998, AJ, 116, 2805
Veilleux, S., Cecil, G., & Bland-Hawthorn, J. 2005, ARA&A, 43, 769
Venn, K. A., Tolstoy, E., Kaufer, A., Skillman, E. D., Clarkson, S. M., Smartt, S. J., Lennon, D. J., & Kudritzki, R. P. 2003, AJ, 126, 1326
Verde, L., Oh, S. P., & Jimenez, R. 2002, MNRAS, 336, 541
West, A. A. 2005, Ph.D. thesis, Univ. Washington
White, S. D. M., & Frenk, C. S. 1991, ApJ, 379, 52
Woosley, S. E., & Weaver, T. A. 1995, ApJS, 101, 181
Zaritsky, D., Kennicutt, R. C., Jr., & Huchra, J. P. 1994, ApJ, 420, 87